Deliverable D.T1.2.3
Report of HS concentrations and loads in the pilot regions
Date: 2023-03-31

AUTHORS AND CONTRIBUTING PARTNERS

Name co-author	Contributing partner
Adrienne Clement	Budapest University of Technology and Economics, HU
Zsolt Jolankai	Budapest University of Technology and Economics, HU
Mate Kardos	Budapest University of Technology and Economics, HU
Ildikó Musa	Budapest University of Technology and Economics, HU
Katalin Maria Dudas	Budapest University of Technology and Economics, HU
Nikolaus Weber	TU Wien, AT
Ottavia Zoboli	TU Wien, AT
Matthias Zessner	TU Wien, AT
Steffen Kittlaus	TU Wien, AT
Dimitar Mihalkov	Bulgarian Water Association, BG
Radoslav Tonev	Bulgarian Water Association, BG
Silviya Petkova	Bulgarian Water Association, BG
Radmila Milacic	Jozef Stefan Institute; SI
Katarina Marković	Jozef Stefan Institute; SI
David Kocman	Jozef Stefan Institute; SI
Elena Tuchiu	National Administration "Romanian Waters", RO
Elvira Marchidan	National Administration "Romanian Waters", RO
Corina Boscornea	National Administration "Romanian Waters", RO
Carmen Hamchevici	National Administration "Romanian Waters", RO
Daniel Luta	National Administration "Romanian Waters", RO
Constanta Moldovan	National Administration "Romanian Waters", RO
Gabriela Ciocan	National Administration "Romanian Waters", RO
Ramona Curelea-Marin	National Administration "Romanian Waters", RO
Florentina Soare	National Administration "Romanian Waters", RO
Monica Mainerici	National Administration "Romanian Waters", RO
Mugurel Sidau	National Administration "Romanian Waters", RO

CONTENT

ABBREVIATIONS

CHEMICAL SUBSTANCE ABBREVIATIONS

Abbreviation	Name	CAS number
Metals		
Cr	Chromium and its compounds	7440-47-3
Ni	Nickel and its compounds	7440-02-0
Cu	Copper and its compounds	7440-50-8
Zn	Zinc and its compounds	7440-66-6
As	Arsenic and its compounds	7440-38-2
Cd	Cadmium and its compounds	7440-43-9
Pb	Lead and its compounds	7439-92-1
Hg	Mercury and its compounds	7439-97-6
Al	Aluminium and its compounds	7429-90-5
Fe	Iron and its compounds	7439-89-6
La	Lanthanum	7439-91-0
Ce	Cerium	7440-45-1
PAHs		
Naph	Naphthalene	91-20-3
Ace	Acenaphthene	83-32-9
Acy	Acenaphthylene	208-96-8
Fluo	Fluorene	86-73-7
Ant	Anthracene	120-12-7
Phen	Phenanthrene	85-01-08
Fla	Fluoranthene	206-44-0
Pyr	Pyrene	129-00-0
BaA	Benzo(a)anthracene	56-55-3
Chry	Chrysene	218-01-9
BbF	Benzo(b)fluoranthene	205-99-2
BkF	Benzo(k)fluoranthene	207-08-9
BaP	Benzo(a)pyrene	50-32-8
DahA	Dibenzo(a,h)anthracene	53-70-3
BghiP	Benzo(g,h,i)perylene	191-24-2
Ind123cdP	Indeno(1,2,3-cd)pyrene	193-39-5
16-PAH_EPA	Sum of the 16 US-EPA PAHs	
PFAS		
PFPeA	Perfluoropentanoic acid	2706-90-3
PFHxA	Perfluorohexanoic acid	307-24-4
PFHpA	Perfluoroheptanoic acid	375-85-9
PFOA	Perfluorooctanoic acid	335-67-1
PFNA	Perfluorononanoic acid	375-95-1
PFDA	Perfluorodecanoic acid	335-76-2

Abbreviation	Name	CAS number
PFUnDA	Perfluoroundecanoic acid	2058-94-8
PFDoDA	Perfluorododecanoic acid	307-55-1
PFTrDA	Perfluorotridecanoic acid	72629-94-8
PFTeDA	Perfluorotetradecanoic acid	376-06-7
PFBS	Perfluorobutane sulfonic acid	375-73-5
PFHxS	Perfluorohexane sulfonic acid	355-46-4
PFOS	Perfluorooctane sulfonic acid and its derivatives	1763-23-1
Phenols		
BpA	Bisphenol A	80-05-07
OP	Octylphenol (4-(1,1',3,3'-tetramethylbutyl)- phenol)	140-66-9
4-NP	4-nonylphenol	104-40-5
Pesticides		
Met	Metolachlor	51218-45-2
Met-ESA	Metolachlor ESA	171118-09-5
Met-OA	Metolachlor OA	152019-73-3
Met_SUM	Sum of the above three	
TCZ	Tebuconazole	107534-96-3
Pharmaceuticals		
CBZ	Carbamazepin	298-46-4
DCF	Diclofenac	15307-86-5

FURTHER ABBREVIATIONS

AD – atmospheric deposition
Dis – dissolved (filtered) concentrations (in river)
EC – electric conductivity
FNU - formazin nephelometric unit, a measure for turbidity
HM – heavy metals, including As
IWW – industrial wastewater
MWW – municipal wastewater
NTU - nephelometric turbidity unit – another measure for turbidity
PAH – polycyclic aromatic hydrocarbons
PFAS – per- and polyfluoroalkyl substances
PTE – potentially toxic elements
RIV – concentration measured in river water
SPM – suspended particulate matter
Tot – total concentrations (in river)
TSS – total suspended solids
WW – wastewater
WWTP – wastewater treatment plant

1 MONITORING RESULTS

For the sake of processing the measurement data provided by the laboratories (i.e. the concentration values), we have imported them to R programming environment (R Core Team, 2019). Throughout this chapter, wherever the term “mean value” or “average value” appears, it can mean two different things: (a) the expected value (numerical mean) of the observed uncensored (i.e. > LOQ) values if the number of uncensored elements n<3 or the detection frequency in the particular class (category) <= 20% and or (b) mean of the statistically modelled (reproduced) multitude otherwise. Statistical modelling was done as described in (Helsel, 2012) using the NADA R package, assuming lognormal distribution of the data. PFOA-equivalents are calculated as the sumproduct of the 12 PFAS values measured in this study and their respective relative potency factor values as proposed in Annex V. of (EC, 2022).

1.1 CONCENTRATION OF ALL SUBSTANCES ACROSS PATHWAYS IN THE PILOT REGIONS

Metals

Except for Cd, all analyzed metals were **detected** in practically all RIV Tot, AD, MWW, samples (Figure 1.1-1); all analyzed metals were detected in almost all (>95%) IWW, Mining and soil samples. Some metals were not detected in a smaller part of RIV Dis samples: Zn, Cd and Pb was missing from 18, 71 and 46% of the samples, respectively. Cd was missing from 48, 11 and 48% of the RIV Tot, AD and MWW samples, respectively.

By far the highest **concentrations** of HM were found in mining drainages: For Zn and Cu in the range of mg/l, but for As, Cd, Ni and Pb also in the range of 100 µg/L.

The second most contaminated matrix is usually head to head river water & WW effluents. River water samples cover the widest range of concentrations for all PTEs; however, some extremely high values as outliers outreach concentrations measured in wastewaters (in case of As, Cr, Cu, Ni, Pb, Zn). Dissolved concentrations in river water are usually significantly lower (for all compounds) or even one order of magnitude lower than total concentrations (Cr, Ni, Cu, Pb, Hg). The lowest concentrations can be found in atmospheric deposition samples and filtered river samples. For AD, orders of magnitude are 10 µg/l for Zn, 1 µg/l for Cu and As, 0.1 µg/l for Cr, Ni, Pb; 0.01 for Cd and 0.001 µg/L for Hg.

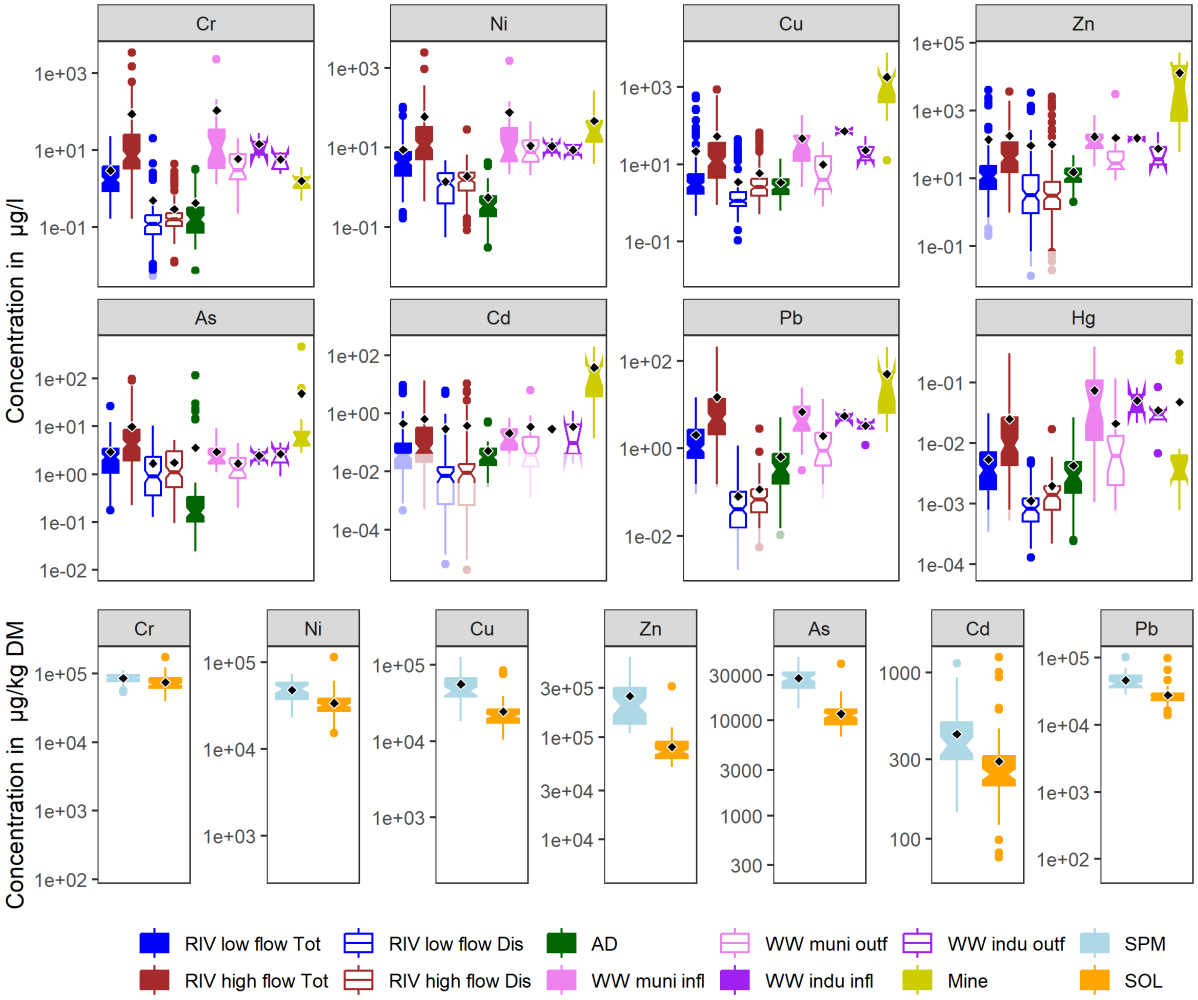

*Figure 1.1-1 - Concentration of HMs across aqueous (top) and solid (bottom) pathways. Notches in the boxplot show 1.58 * IQR / sqrt(n) which is roughly the 95% CI of the median. Lighter colours at the bottom of a bar indicates ROS-modelled values. Black diamonds represent calculated mean values.*

In soil samples, Zn and Cr exhibited the highest concentrations (51.3 – 313 and 39.3 - 174 mg/kg DM, respectively). Concentration of Ni, Pb, Cu and As was an order of magnitude lower: between 15.2 – 115, 13.9 – 98, 10.4 - 84.2 and 6.78 - 39.5 mg/kg DM, respectively. The lowest concentration range was exhibited by Cd (0.077 - 1.24 mg/kg DM).

PAHs

Only Naph, Phen and Fla **occurred** in more than 50% of the RIV samples whereas the 8 PAHs with 18 or more C atoms (BaA, Chry, BbF, BkF, BaP, BghiP, Ind123cdP and DahA) occurred in <10% of the RIV samples (Figure 1.1-2). A similar but less contrast picture is shown by AD samples: Naph, Phen, Fla, Pyr occurred in >50% of the samples whereas the larger compounds in only 20-40% of the samples. Only Naph and Phen was found in substantial share (75-90%) of the MWW samples, and Ace and Fluo in a few (19%) of them. Only Naph and Phen was found in IWW samples. Naph, Ace, Fluo, Phen and Fla taught up in Mining effluent samples with a wide range of occurrence ratio ranged from 100% for the 2-ring Naph to 30% for the 4-ring Fla. Here again hydrophobicity might be an explanation, but – in case of IWW – the particular activity also determines the composition of the WW. For soil, the situation is

reverse: higher molecular weight (>200) and higher ring number (>= 4) compounds like Fla, Pyr, BaA, Chry, BaP, BbF, BkF, BghiP, Ind123cdP and DahA are almost ubiquitous (usually >90%) whereas compounds with 2-3 rings were rare to occur (in 3-46% of the samples).

Highest mean **concentrations** of ∑PAH16 were measured in MWW and AD (0.0636 +/- 0.079 µg/l and 0.0606 +/- 0.0583 µg/l, respectively), followed by Mining, RIV and IWW samples (0.15 +/- 0.176, 0.0254 +/- 0.0306 and 0.0182 ± 0.0124 µg/l, respectively) which underlines the fact that these substances are really ubiquitous, reaching surface waters through many pathways.

Concerning soil samples, mean concentration of ∑PAH16 in forest soils exceeded those in agricultural and pasture soils (84.2 vs 63 and 49.8 µg/kg, respectively). In agricultural soils, the upper 25 cm of the soil is frequently mixed during tilling operations (where applied) therefore the concentrations in the tilled layer is evened out. It is however contradictory that in pasture soils, where the sampling was carried out in the same horizon as for the forest soils, the PAH concentration are significantly lower.

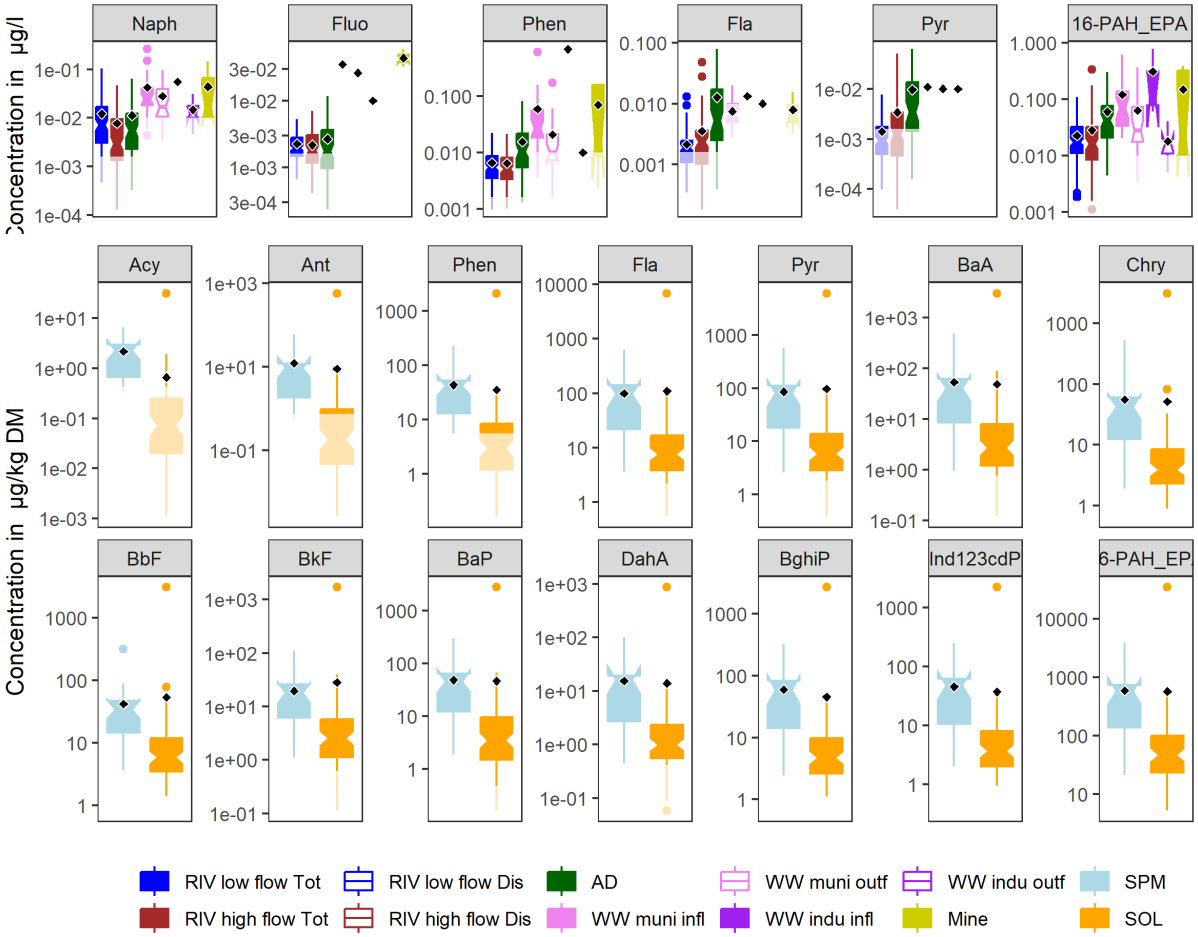

*Figure 1.1-2- Concentration of PAHs across aqueous (top) and solid (bottom) pathways. Notches in the boxplot show 1.58 * IQR / sqrt(n) which is roughly the 95% CI of the median. Lighter colours at the bottom of a bar indicates ROS-modelled values. Black diamonds represent calculated mean values.*

PFAs

When investigating the detection rates of the PFAs attention has to be given to the fact that LOQ for PFOS and PFOA in aqueous matrices was one order of magnitude lower than for other

PFAs. The two PFAs produced traditionally in the greatest volumes (PFOA and PFOS) were found in 80 and 60% of the river samples, respectively. From the other PFAAs, shorter (5-7) chain acids and sulfonates were **detected** in 7-35% of the river samples whereas longer chain acids were completely missing from all aqueous samples. Regarding atmospheric deposition, PFOA was detected izn 92% of the samples whereas PFOS in 19% of the samples; PFHpA in 8% of the samples. Similar holds for both municipal and industrial waste waters: PFOA could be quantified in 63-33%, whereas PFOS in 41-17% of the samples, respectively, but no other compounds occurred in substantial share of the samples. No PFAAs were found at all in mining effluent waters.

Soil is somewhat different: except for the very long chain (n>13) compounds, each substance was detected in soils (Figure 1.1-3). The detection rate decreases with the increase of the chain length (from 100% for pentanoic … nonanoic acid to 39% for dodecanoic acid). Seemingly, soil is an accumulator of these substances, and shorter chain substances occur more often. (Gao et al., 2019) also observed that shorter chain PFAAs have higher detection frequencies.

River **concentrations** (Figure 1.1-3) were between <0.00015 - 0.0187 and <0.00015 - 0.0162 µg/L for PFOA and PFOS, respectively. Regarding metabolites and precursors, the concentration of shorter chain acids and shorter chain sulfonates was <0.002 – 0.02 and <0.02 – 0.018 µg/l, respectively. Atmospheric deposition had concentrations of <0.00015 - 0.00113 and <0.00015 - 0.00733 for PFOA and PFOS. WW concentrations ranged between <0.0015 – 0.0049 and <0.0015 – 0.0219 µg/l for PFOA and PFOS, respectively. Soil concentrations were between 0.005 - 1.21 and 0.01 - 0.383 µg/kg DM for PFOA and PFOS, respectively. Regarding metabolites and precursors (n = 5-7, 9-10), the concentration was between 0.006 – 0.68 µg/kg. PFAA concentrations in soils show heterogeneity across land uses. The total concentrations of the 13 analyzed variants for all soils were in the range of 0.093-4.231 mg/kg with means of 0.371, 1.101 and 0.699 mg/kg for agricultural lands, forests and pastures, respectively. The highest average concentrations were found for perfouroctanesulfonic acid (PFOA) with 0.087, 0.246 and 0.147 mg/kg for agricultural, forest and pasture soils respectively. PFOA was followed by PFPeA and PFOS and the distribution between the land uses was similar, with highest values for forest followed by pasture and agricultural lands.

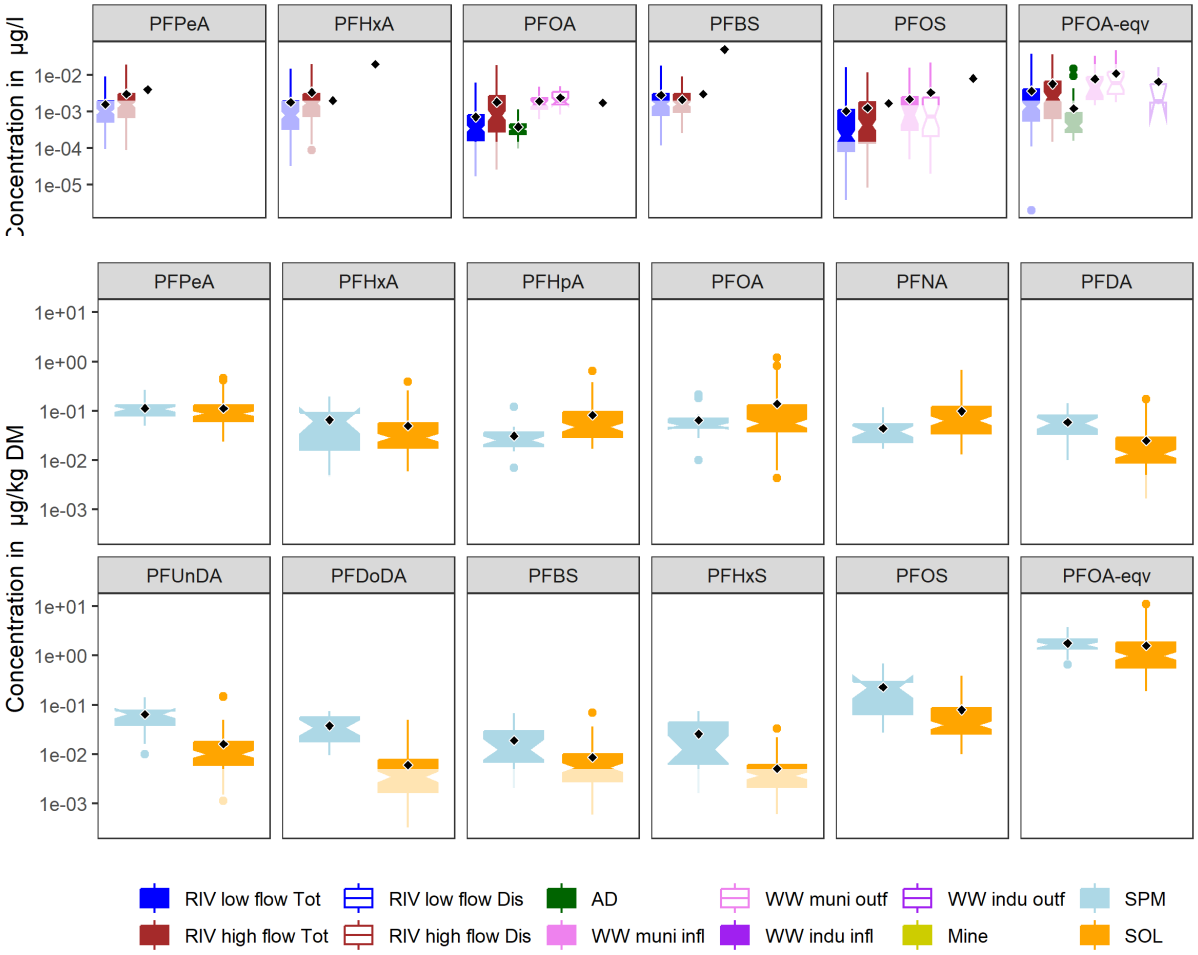

*Figure 1.1-3 - Concentration of PFAs across aqueous (top) and solid (bottom) pathways. Notches in the boxplot show 1.58 * IQR / sqrt(n) which is roughly the 95% CI of the median. Lighter colours at the bottom of a bar indicates ROS-modelled values. Black diamonds represent calculated mean values.*

Phenols, Pesticides & Pharmaceuticals

Out of the three phenols, Nonylphenol was not **detected** in any of the samples. No soil sample exhibited measurable concentration of any phenols. BpA occurred in ~65% of the AD and IWW samples and in smaller share (26-35%) of the MWW and RIV samples but was missing from Mining effluents. OP occurred in 50% of the Mining effluent samples(!) and in smaller share (5-15%) of the AD, RIV and MWW samples but was missing from IWW samples.

D**etection** frequency of both the original pesticides was higher in high flow than in low flow (35% vs 10% and 36% vs 12% for Met and TCZ, respectively). In contrary, the two metabolites could be detected in less or equal low flow samples than high flow samples (49% vs 49% and 41% vs 44% for Met-ESA and Met-OA, respectively). This underlines the process of degradation with time: low flow samples reached the monitoring locations with substantially longer travel times which allowed them to transform. Detection in AD and soil is in line with that in high flow: 33 - 36% and 10-13% for Met – TCZ in AD and soil, respectively. While no pesticide was detected in Mining effluents, there were a few detects of metabolites in municipal and industrial WW effluents (4 and 2 detects, respectively). Met and TCZ could be

detected in 10 and 13% of the soil samples, respectively whereas detects of metabolites was neglectable.
Both CBZ and DCF were **detected** in all MWW samples and 82-84% of IWW and RIV samples. Surprisingly, they were also found in part of the AD samples (8 and 38% for CBZ and DCF, respectively). As expected, pharmaceuticals were not detected in Mining effluents and soil.

C**oncentrations** of BpA (**Hiba! A hivatkozási forrás nem található.**) ranged from 28.9 / 5.07 (maximum / mean conc., respectively) in IWW to 0.29 / 0.018 µg/l (maximum / mean conc., respectively) in RIV. Mean / maximum concentration of OP in the mining effluents of the Viseu catchment was 0.09 / 0.034 µg/l.

Maximum Met **concentration** was 80, 0.8 and 0.21 in high flow, low flow and AD, respectively; maximum TCZ concentration was 2, 0.06 and 0.11 in high flow, low flow and AD, respectively. Max / mean concentration was 4.02 / 0.176 and 0.28 / 0.049 for Met-ESA whereas 6.74 / 0.214 and 0.21 / 0.021 for Met-OA in river high flow and low flow, respectively, indicating that concentrations of both pesticides as well as their metabolites are about one order of magnitude lower in high flow samples than in low flow samples. Concerning pesticides concentrations, there is a substantial difference however within pilot regions. There are only 3 pilots, where the detection frequency of any pesticide in river water fell above 20%: Wulka, Koppány and Zagyva (Figure 1.1-4). In addition, detection frequencies for metabolites were above 20% on the Ybbs, Somes and Vit catchments, too, with the above-mentioned regularity that these substances have in most of the cases lower detection frequencies in high flow than in low flow.

The highest **concentrations** were measured in MWW and IWW samples followed by RIV and AD. Maximum / median RIV concentrations were 1.33 / 0.0425 and 1.99 / 0.0555 µg/L for CBZ and DCF, respectively. AD samples containing CBZ originate from the Zagyva, Somes and Viseu catchments, whereas samples containing DCF cover all pilot areas. Maximum / mean concentration of CBZ and DCF in AD samples was 0.02 / 0.0064 and 0.313 / 0.0082 µg/L respectively.

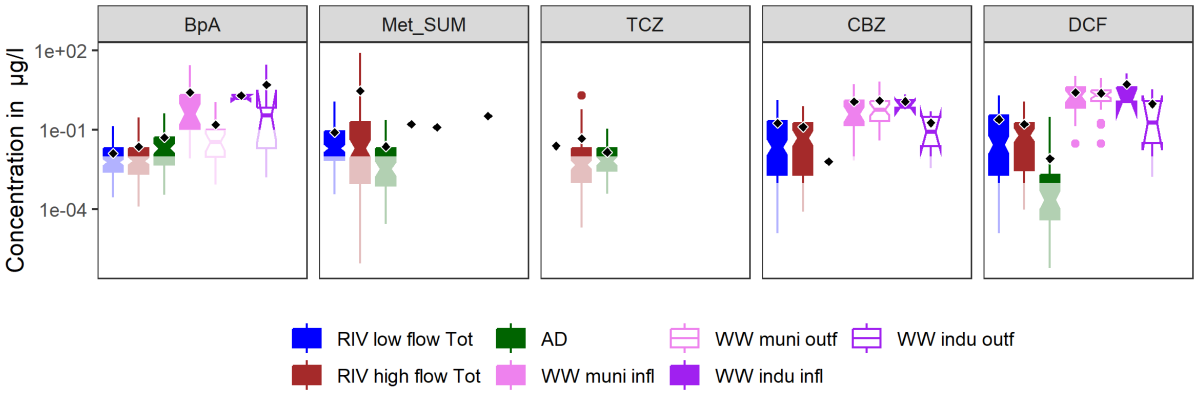

*Figure 1.1-4 - Concentration of BpA, pesticides and pharmaceuticals across aqueous (top) pathways. Notches in the boxplot show 1.58 * IQR / sqrt(n) which is roughly the 95% CI of the median. Lighter colours at the bottom of a bar indicates ROS-modelled values. Black diamonds represent calculated mean values.*

1.2 CONCENTRATIONS ACROSS PILOT REGIONS / COUNTRIES

River water

Metals

As already stated, mining activities exhibit the highest concentration of metals. This is also reflected in the river concentrations of the Viseu catchment (both low and high flow, both total and dissolved concentrations) in particular for Cu, Zn and Cd. Metals are known for their affinity to adsorb on small particles, which explains the elevated concentration of total metals during high flow events. The reason for this phenomenon being less pronounced on the last three catchments (Somes, Viseu and Vit) is that in these three catchments, the difference between actual river flow during collection of high flow vs low flow samples was small (i.e. we did not manage to catch really good high flow events). The elevated As concentration of groundwaters in the Pannonian region (Giménez-Forcada et al., 2022) are reflected by the dissolved As concentrations in river water. The most pristine water of the alpine catchment Ybbs are reflected by the lowest dissolved Pb concentrations in low flow samples (Figure 1.2-1.).

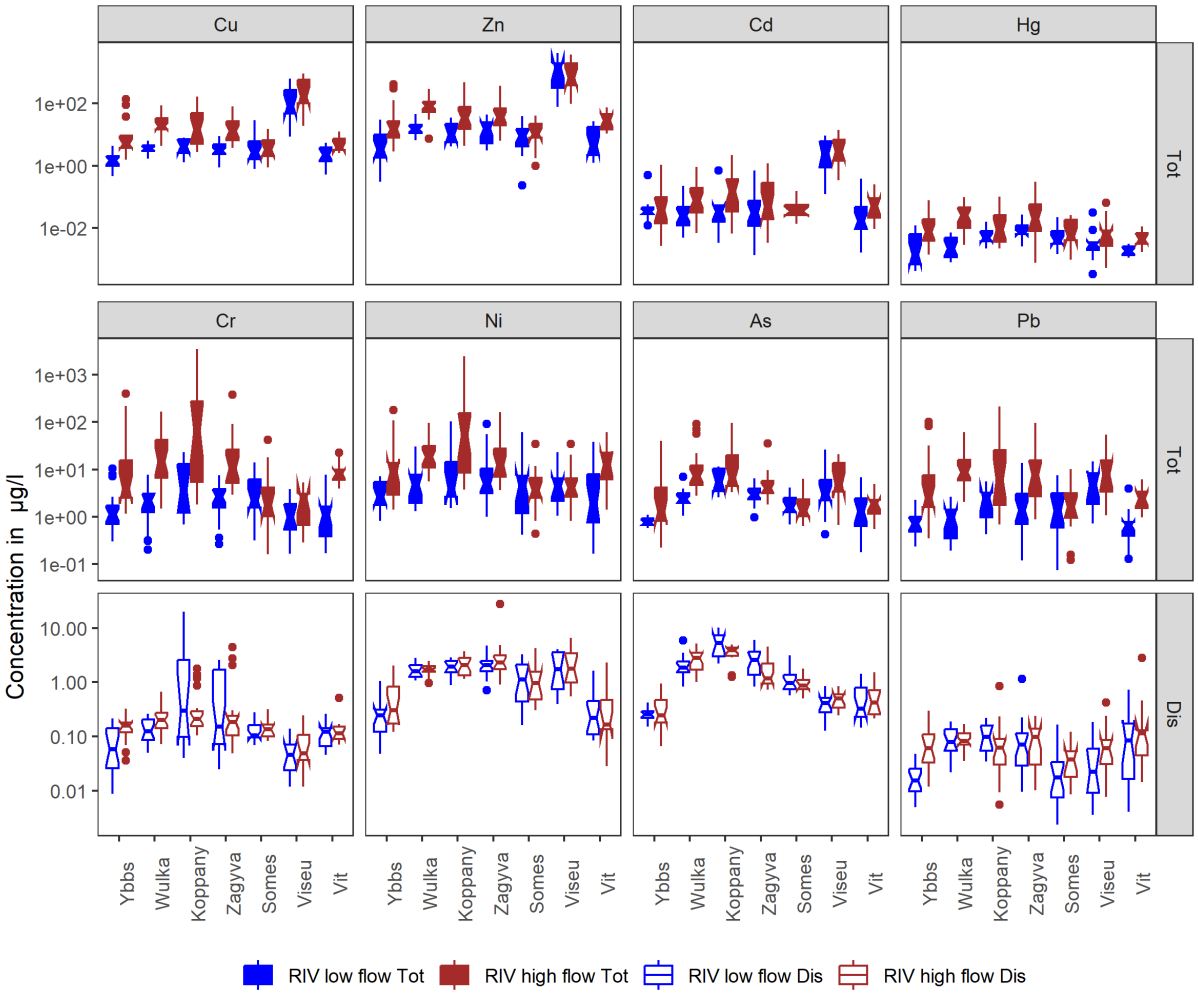

Figure 1.2-1 - Concentration of HMs across pilot regions. *Notches in the boxplot show 1.58 * IQR / sqrt(n) which is roughly the 95% CI of the median.*

PAHs

Behaviour of **PAHs** is fuzzy for the first glimpse and thus worth for investigation. Regarding the bunch of the PAs, there is no real difference between low flow and high flow concentrations of the 6 main PAHs that were detected in surface waters, although Naph is somewhat diluted (has lower concentrations in high flow) while Pyr is somewhat concentrated during high flow events. In particular, ratio of high flow to low flow median and mean values are between 41 - 64% for Naph and Ace, between 92 – 98 % for Fluo and Phen while between 124 – 241% for Fla and Pyr. This clearly indicates, that the higher molecular weight, ring number and hydrophobicity compounds tend to associate more to particles and thus enrich during high flow events. The bunch investigation, however, masks some spatial patterns which is most visible when comparing the Wulka and the Koppány catchments. On the Wulka, concentration of ΣPAH and especially Phen is higher in high flow samples than in low flow samples while it is the other way round on the Koppány (ratio of high flow mean to low flow mean Phen values is 1.42 and 0.73 on the Wulka and Koppány, respectively). The reason behind is in the source of the PAHs: on the Wulka, it is more the AD while on the Koppány, it is more the WW (mean Phen concentration in AD / WW is 20.7 / 9.8 and 12.8 / 25.9 ng/l in the Wulka and Koppány catchments, respectively.) From this aspect, the Zagyva and Somes catchments are similar to the Koppány, while the Ybbs, Viseu and Vit catchments show no pattern (Figure 1.2-2).

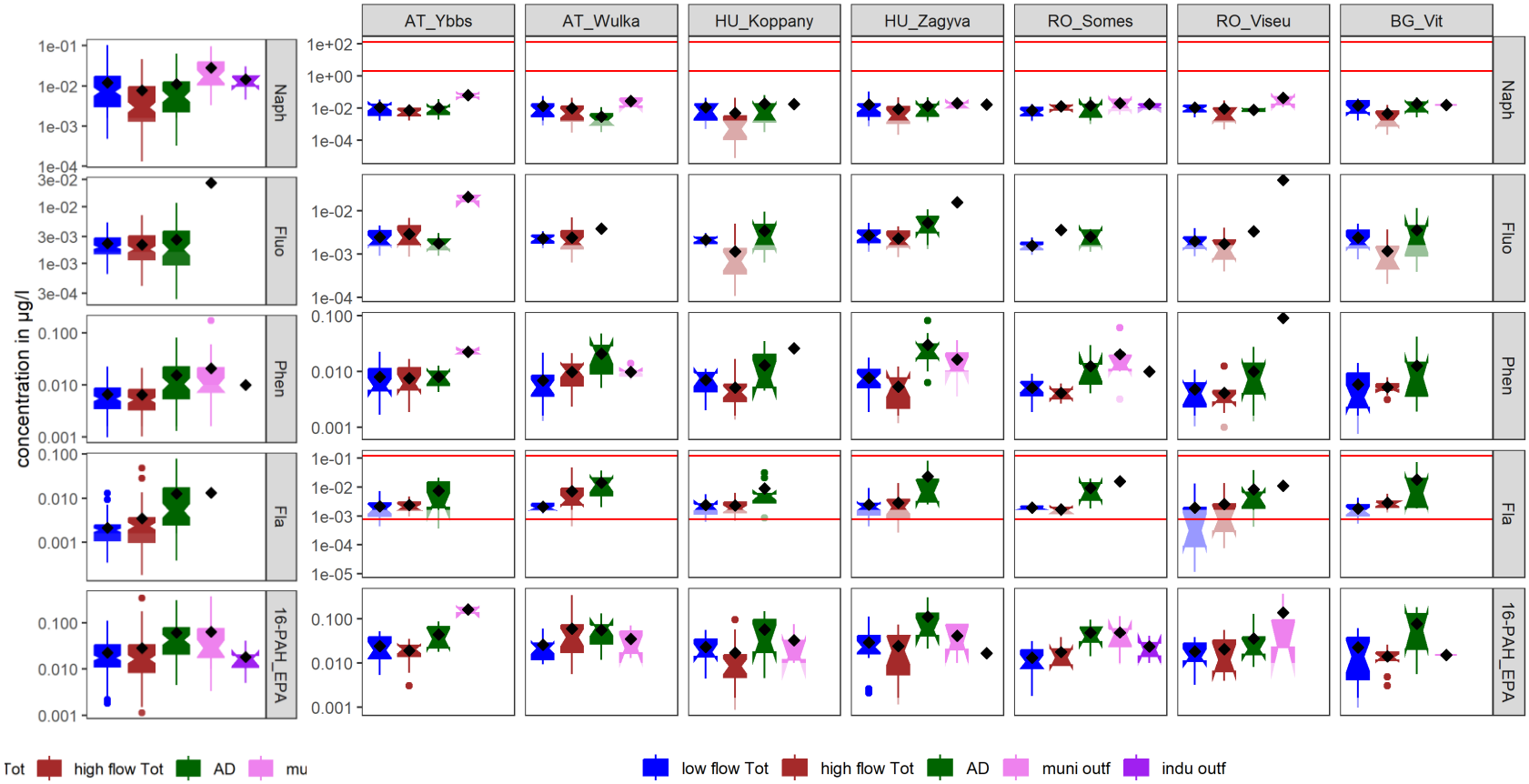

Figure 1.2-2 - Concentration of HMs across pilot regions. *Notches in the boxplot show 1.58 * IQR / sqrt(n) which is roughly the 95% CI of the median.*

Further organic compounds

Regarding PFAS, there is a tendentious difference between carbocyclic acids and sulfonates. While the former thend to have larger concentrations during high flow events than during low flow periods, the latter have slightly lower or same range of concentrations during high and low flow events. Another tendency to be observed the decrease in riverine concentrations for almost many substances when listing the pilots from Wulka to Vit, northwest to southeast. The Ybbs is here however an exeption, it shows ranges of concentrations characteristic for the Hungarian pilots or even lower. A possible explanation lies in the difference in economic development of the pilot areas.

BpA tends to show somewhat higher concentrations during high flow events. This does not hold for the Koppány and the Somes catchments, but the latter are mostly ROS-modelled values and thus uncertain. On the other hand, there is no clear tendency in BpA concentrations across pilot areas. Pesticides were mainly detected on the Austrian and Hungarian pilot regions, - as expected – mainly during high flow events. Pharmaceuticals are expected to be diluted by high flow events, which is partly proven (especially on the Koppány catchment, for both pharmaceuticals). The three Central-European pilot regions (Wulka, Koppány and Zagyva) show somewhat elevated riverine concentrations of the pharmaceuticals compared to the rest of the pilots (Figure 1.2-3).

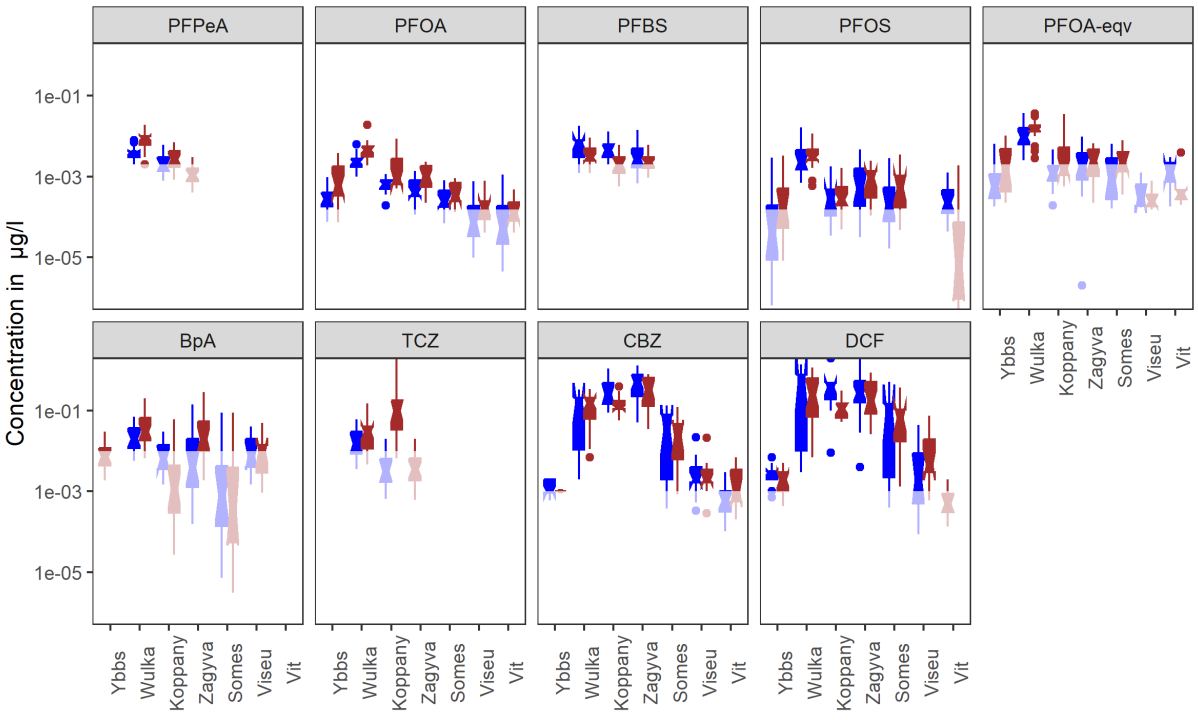

Figure 1.2-3 - Concentration of PFAs and other organic substances in low- and high flow samples across pilot regions. Blue: low flow; brown: high flow samples. Light colours indicate ROS-modelled values.

Waste water

Differences between countries

Number of WW samples is much smaller than those of RIV samples. In addition, regulations for WW vary by country, which has the consequence that it is has more sense to compare WW values by country. Influent concentration of HM are usually larger in Hungary, whereas the tendency in effluent values varies by compound (Figure 1.2-4).

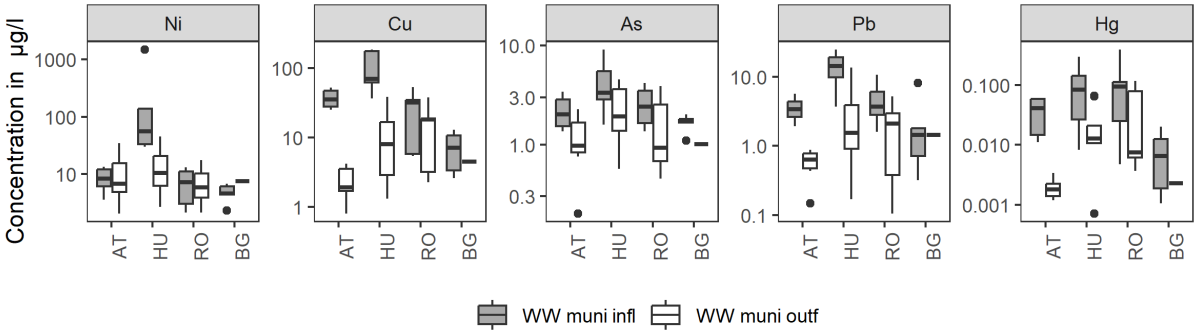

Figure 1.2-4 - Concentration of HM in raw & treated municipal WW samples.

Regarding organic compounds, both in- and effluent concentrations are relatively constant throughout the countries. PAHs are partly removed, especially longer molecular weight ones, most probably because they tend to adsorb to particles. On the contrary, PFOA varies both within and across countries and is not removed at all but it might exhibit slightly higher concentrations in the outflow as in raw WW (see the case of Austria on Figure 1.2-5). Pharmaceutical concentrations are somewhere in between, they show some variance across countries.

There are some outliers in the results. Hungary ,for example, exhibits higher concentration of both pharmaceuticals. The fact that the plant HZS treats wastewaters from a county-scale hospital, only partly explains this anomaly – the underlying process might be the higher consumption of these substances throughout the country but further investigation is needed to underline this statement. Plant HKB showed one order of magnitude higher concentrations of BpA, and somewhat higher concentrations of PFs than other plants, indicating industrial activity on the drained area.

Regarding removal efficiencies, the concentration of some PAH forms and BpA was slightly reduced during treatment (median removal efficiency was 37%, 57% and 89%, for Naph, Phen and Bpa, respectively). Other industrial chemicals as well as pharmaceuticals trespass wastewater treatment practically unaffected (median removal efficiency was -47%, -13%, 13%, -12%, and 25% for PFOS, PFOA, OP, CBZ and DCF, respectively). Negative removal efficiencies for pharmaceuticals might be surprising, but were documented previously, too and are associated with high uncertainties in lab determination of the compounds due to the very low concentrations (Yang et al., 2017) (Figure 1.2-5).

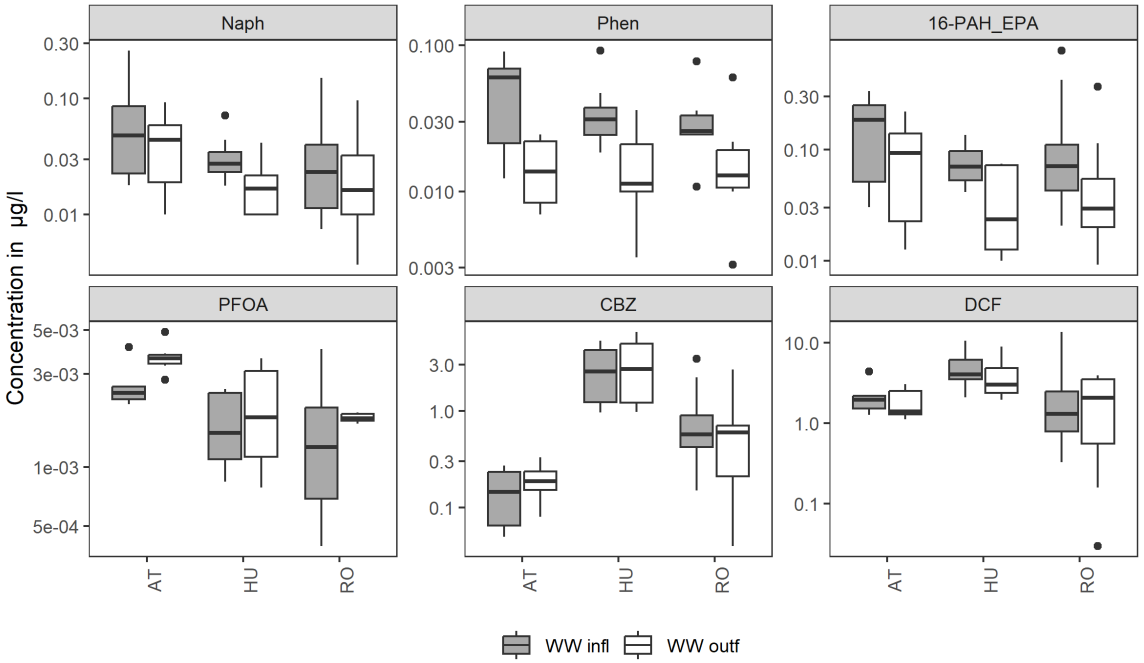

Figure 1.2-5 - Concentration of selected organic pollutants in raw & treated WW samples. Only plants with both in- and outflow samples included (whether municipal or industrial).

Atmospheric deposition

Lowest ∑PAH16 values were shown in the Viseu catchment (25 ng/l at the Viseu de Sus station) while highest ones on the Zagyva catchment (125 ng/l at station Nemti). This can be regarded as a rather narrow range considering the large distances between the stations. There is a difference in the composition of the ∑PAH, however: the biggest contrast can be observed between the Nodbach and the Cluj stations. In the former, low C-number PAHs (Naph, Ace, Fluo, Ant) are missing while in the latter, high C number (C>17) PAHs are missing. Since both stations are more or less situated in developed areas, further investigation is needed to reveal the reason for this difference (Figure 1.2-6).

Measured concentrations can be compared according to the environment in which the stations were located. However, there is no substance for which there would be a significant difference between rural and urban-industrial sites. For most substances, the concentrations range within a rather narrow interval across all sites, but there are a few exemptions. Amount of BpA in atmospheric deposition samples in the Koppány catchment was 1-2 orders of magnitude higher than in other catchments (Figure 1.2-7).

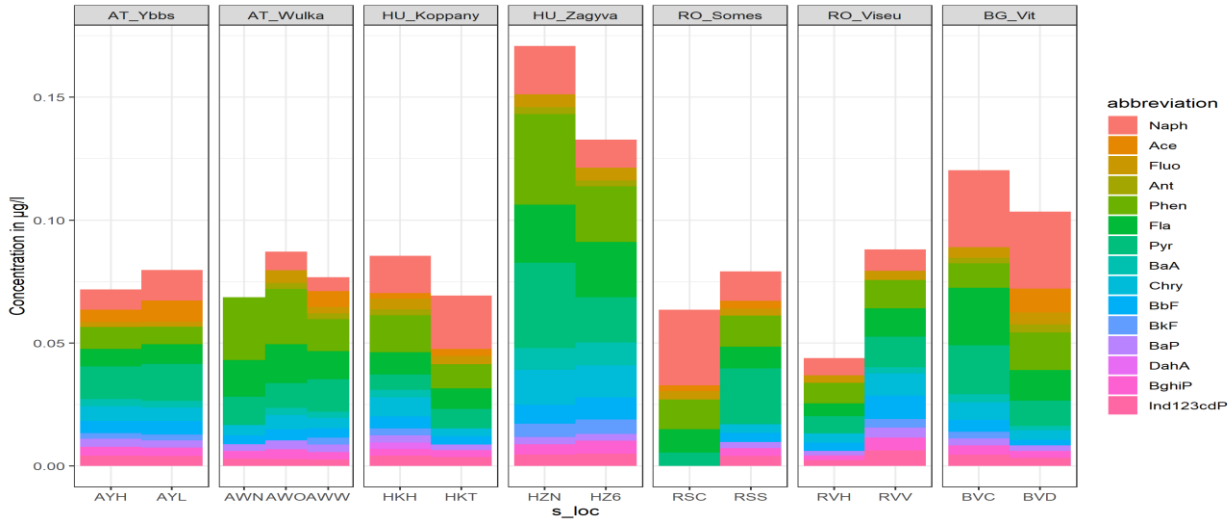

Figure 1.2-6 - Concentration of PAH forms in atmospheric deposition across sampling locations.

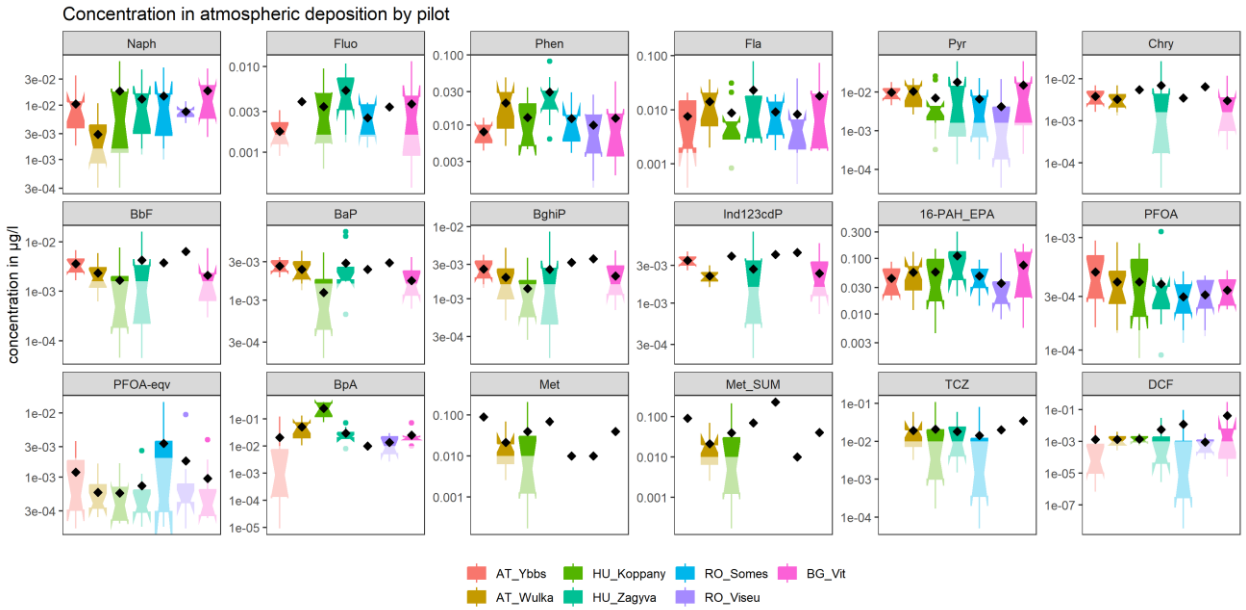

Figure 1.2-7 - Concentration of selected pollutants in atmospheric deposition across pilot regions. Light bottom part of a box denotes ROS-modelled values.

Soil & SPM samples

Soil concentrations are in general much less variable within the catchments then river concentrations. This might be due to the fact that they are composite samples composed from samples originating from 20 locations and thus differences might be levelled out. Cd exhibits the lowest while Cr & Zn the highest concentrations for all pilots, the latter especially for SPM.

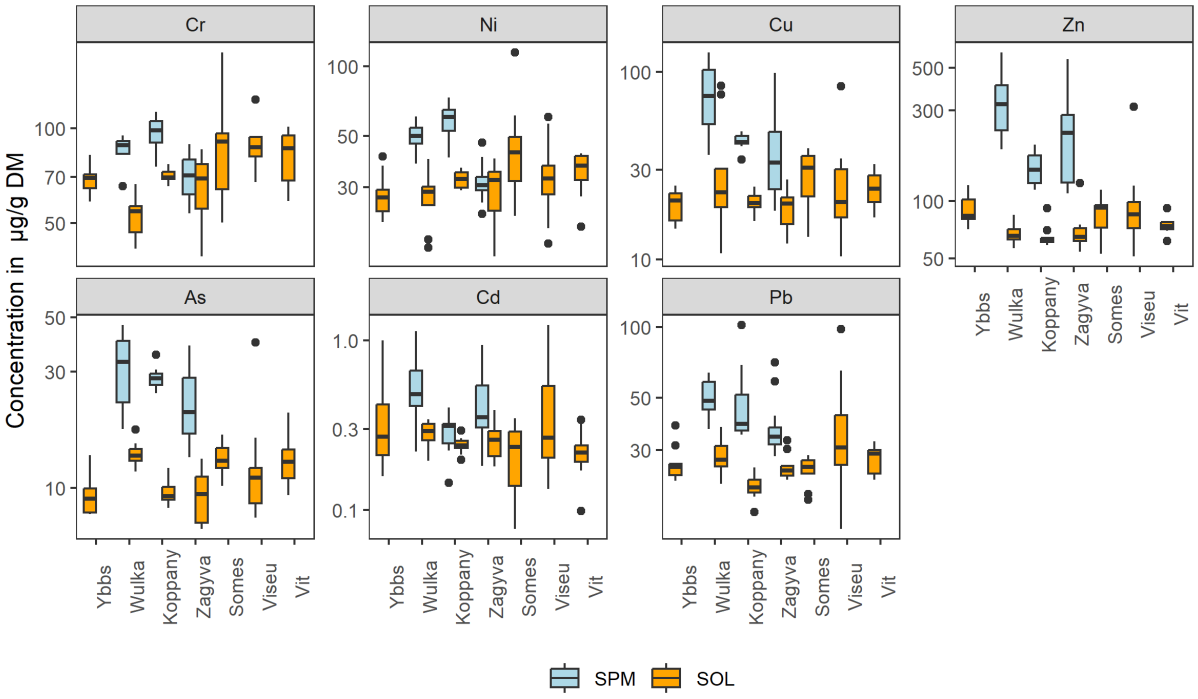

Figure 1.2-8 - HM concentrations in SOIL and SPM samples.

Concentration of Cr, Ni, Cu and Zn is higher in agricultural soils than in forest soils for almost all pilot regions. For As and Cd, it varies; but for Pb, agricultural soils exhibit lower concentrations than forest soils. All PAHs exhibit lower concentrations in agricultural soils than in forest soils in all countries / catchments – except for the Somes. We suspect that these tendencies reflect legacy pollution: high atmospheric concentrations of Pb and PAHs were adsorbed on leaves (forests have leaf area indices much higher then agricultural crops), after falling they became soil. Further investigations could confirm or deny this statement. Both PAH and PFAs, both in forest and agricultural soils decrease in the direction of northwestern to southeastern countries (AT – HU – RO – BG) i.e. their concentration increases with economic development. The only exception is PFPeA, which has higher concentrations in BG agricultural soils, too, probably due to one or more outliers in agricultural soils. The reason for Somes soils as outliers might be the industrial activity in a relatively closed valley (Figure 1.2-8).

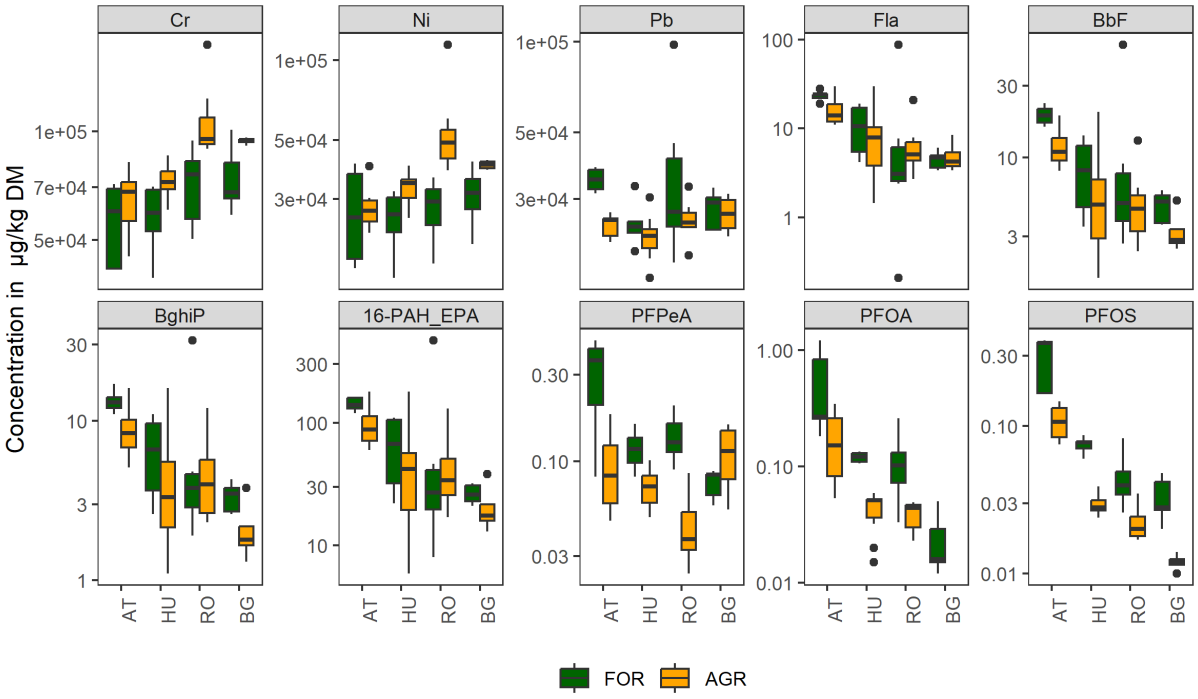

Figure 1.2-9 - Concentration of HM, PAH and PFAs in forest and agricultural soils across the pilot countries.

The spatial pattern across the pilot regions are similar in case of most PAH compounds. Slightly different behaviour and pattern can be identified for DahA, which is in higher concentrations in the Koppány catchment in relative terms to the other substances. There are obviously very high values of PAH concentrations at some pasture and forest samples from the Somes and Viseu catchments; agricultural samples from these two catchments however show concentration ranges comparable to the other pilots (Figure 1.2-9.).

Besides PAH and PFAs, only pesticides were found in detectable amounts in agricultural soils of three catchments. Metolachlor was found in 5 out of 6 agricultural soil samples of the Koppány catchment with an average concentration of 0.1 mg/kg. Tebuconazole, however, was found in all the agricultural soil samples of the Zagyva catchment with an average concentration of 0.055 mg/kg. These occurrences of specific pesticides might be explained by area specific agricultural practices, including the selection of chemicals for application and the timing of the pesticide application due to climatic reasons.

1.3 Concentrations in the Danube River

Interpretation of concentrations measured in the Danube samples is hindered by the diversity of substances measured at the stations and by varying – and in many cases too high – limits of quantification. Still, some trends are to be seen. Most heavy metals have balanced concentrations except for some outliers at specific stations – they might be associated to higher water flow periods, further investigation is needed to confirm this. Higher geogenic arsenic in the Pannonian region is again reflected in somewhat elevated concentrations of As in the Hercegszántó station data (the southern border of Hungary). Higher Pb concentrations

at the Bratislava station might reflect legacy contamination of the industrialized upper-middle regions of the watershed. There is a slight decrease in the concentration of PAHs along the longitudinal section of the river. Highest PFOA levels were measured at both Croatian stations (Batina, Ilok). A possible explanation is that countries located in the middle part of the watershed are in the economic situation to purchase PF-containing clothing and accessories but not aware enough of the risks to try to avoid them. Lower PFAS-levels close to the mouth might either be related again to the economic situation or to the removal of these substances with SPM settling above the Iron Gate. Concentration of both pesticides is lower on the upper sections compared to the lower sections suggesting that these chemicals are still in use in the southern and eastern part of the watershed. Both pharmaceuticals could be detected and quantified in each section and show rather homogeneous concentrations. Further investigations, and – first and foremost – a strict interlaboratory comparison and evaluation is needed to confirm and reject the above speculations (Figure 1.3-1).

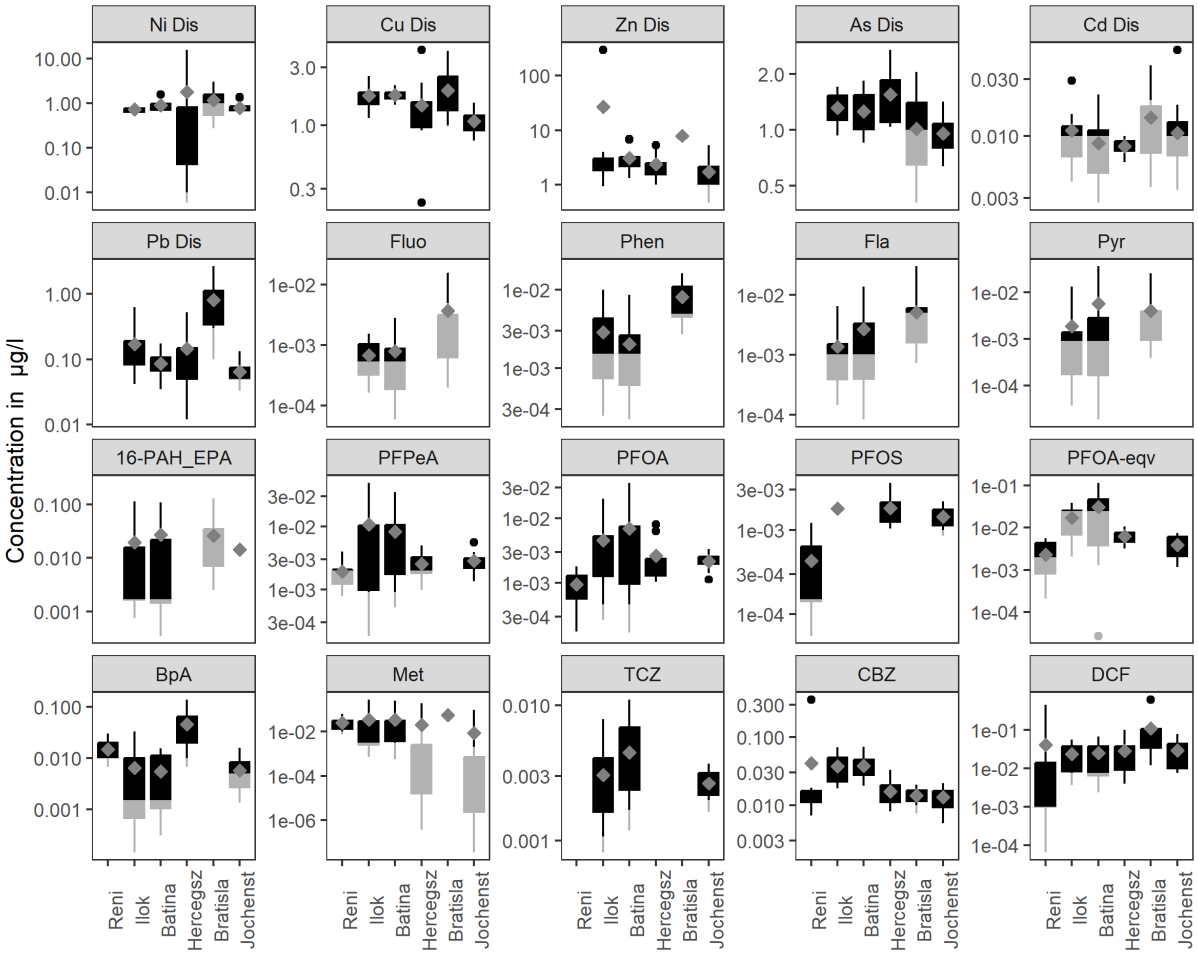

Figure 1.3-1 - Concentration of various substances along the Danube River. Dis = dissolved (filtered) portion. Grey diamonds show mean values. Grey part of the boxes and whiskers show ROS-modelled values.

2 LOAD CALCULATION

2.1 INTRODUCTION TO THE AIMS AND CONCEPT

The necessity of load estimations is rooted in the approach to how catchment scale estimation of hazardous substances are dealt with. Proper estimation of sources and the identification of pathways related to individual chemicals can be best delivered with emission models. These models however can be only calibrated and validated by mass fluxes of the substances in other words loads. The estimation of annual loads have several ways, in most cases loads are calculated based on frequent discharge data and temporally scarse water quality data (e.g. 12 measurements per year). Using such data leads to large estimation errors, especially due to the largely nonlinear characteristics of river flows and therefore, also of river loads. To overcome this problem a stratified sampling approach have been initiated in the DHm3c project, where loads associated with baseflow conditions and highflow conditions are separately addressed in the monitoring. In this chapter the applied data processing and load calculation methods are described, followed by the introduction of the load calculation results, leading to conclusions about the viability of the approach.
Throughout the chapter on load calculation, following terms are used:

Table 1 - Terminology

Load	Mass flux of the given HS at a river section [M/T]
River flow	Water flux through a river cross section
Flow condition	River river flow is classified into baseflow and eventflow.
Baseflow	River flow which occurs most of the time throughout the year (Low- to mid-flow(MQ))
Eventflow	River flow which exceeds baseflow (caused by rainfall or snowmelt)

All calculations were done using the statistical software R (Version 4.2.2) (Everitt & Hothorn, 2003; R Core Team, 2019)

We used a time window of 1 year which corresponded with the sampling dates of the low flow samples. An example can be seen in the following plots:

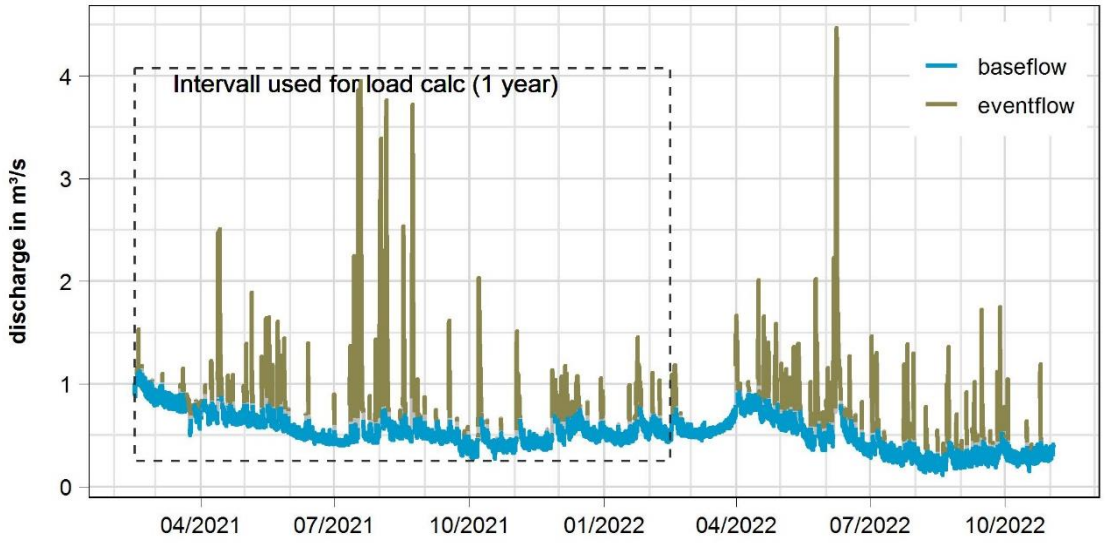

Figure 2.1-1 - - River flow timeline of Wulka river with colour according to flow condition. Dashed box show the interval used for the load calculation (1 year).

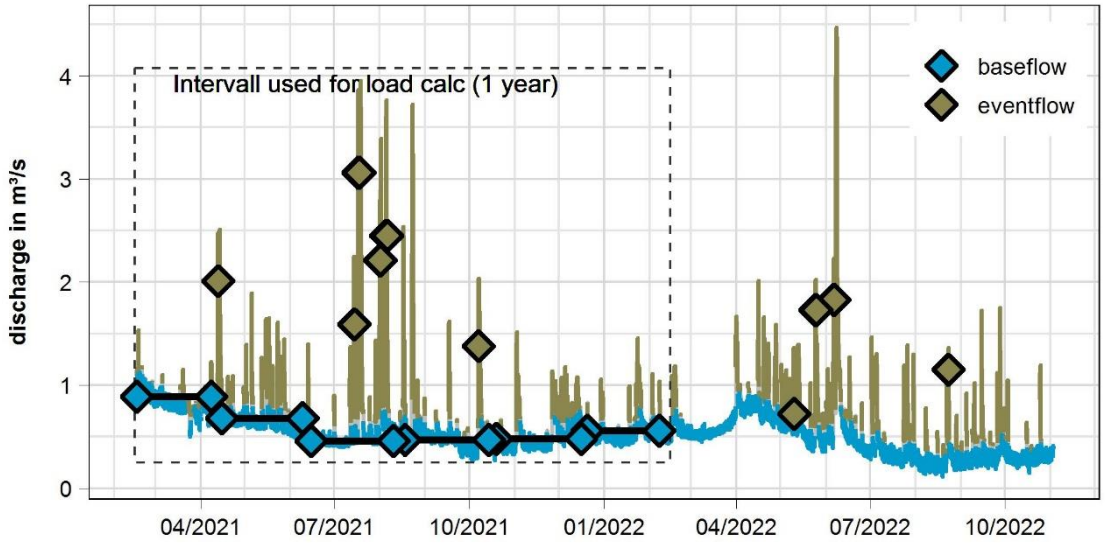

Figure 2.1-2 - River flow timeline of Wulka river with colour according to flow condition. Dashed box show the interval used for the load calculation (1 year). Diamonds show the composite samples used for concentrations data. Fill colour indicate flow condition, distance between diamonds show time between first and last sample and height on y-axis show mean river flow during sampling.

The load was calculated for each station, each substance, each matrix type (total or filtered).

2.2 FLOW DATA PROCESSING, BASEFLOW SEPARATION

River flow data is available for each of the 20 monitoring stations out of the 7 DH m³c pilot regions. How this data was collected can be found in the pilot site description (Output O.T1.2 – Annex AI).

Timesteps of continuous measurement data collected at the online stations vary between 30 secs. and 1 h.

The river flow data was aggregated into 1 h timesteps (mean) and gaps in the timeline (max. 2 timesteps) were filled by linear interpolation. For this calculation step the R package "DTSg" was used (Hepp, 2022). The data series is reduced to a length of 1 year in order to calculate representative annual loads. The collection of the water samples is mostly within this period.

To separate the river flow into the two flow conditions, the Lynne-Hollick (LH) baseflow filter from the R package "hydrostats" (Version 0.2.4) is used (Bond, 2022; Ladson et al., 2013). The package's „baseflow" function with all their default values is used.

Because the baseflow value (BF), calculated by the filter, is only the lower threshold of river river flow, it must be increased by a (constant or variable) value to include the observed variability of the rivers baseflow (see Figure 2.2-1). As each river behaves differently, a factor (threshold_factor) was introduced to fit the method to each river dataset. The individual threshold factor for each monitoring station can be found in Table 2. One of the following two formulas is used to calculate the separation threshold in m³/s:

- Constant threshold: separation_threshold = BF + mean(BF * threshold_factor)
- Variable threshold: separation_threshold = BF + BF * threshold_factor (for stations: "DH-RIV-HKH" & "DH-RIV-HZ6")

Table 2 - Threshold factor for each station used for the flow separation method

COUNTRY	PILOT REGION	STATION NAME	TF
AT	AT Wulka	DH-RIV-AWM	0.4
AT	AT Wulka	DH-RIV-AWE	1
AT	AT Wulka	DH-RIV-AWN	0.9
AT	AT Ybbs	DH-RIV-AYU	1.4
AT	AT Ybbs	DH-RIV-AYL	1
AT	AT Ybbs	DH-RIV-AYH	0.7
HU	HU Koppany	DH-RIV-HKH	0.7
HU	HU Koppany	DH-RIV-HKT	0.1
HU	HU Zagyva	DH-RIV-HZH	0.7
HU	HU Zagyva	DH-RIV-HZ6	0.3
HU	HU Zagyva	DH-RIV-HZT	1
HU	HU Zagyva	DH-RIV-HZN	0.8
BG	BG Vit	DH-RIV-BVB	0.4
BG	BG Vit	DH-RIV-BVC	0.1
BG	BG Vit	DH-RIV-BVD	0.3
RO	RO Viseu	DH-RIV-RVV	0.4
RO	RO Viseu	DH-RIV-RVC	0.4
RO	RO SomMic	DH-RIV-RSU	0.3
RO	RO SomMic	DH-RIV-RSD	0.3
RO	RO SomMic	DH-RIV-RNR	0.3

The final separation of river flow into flow condition was done by the following condition:
River flow <= separation_threshold -> baseflow
River flow > separation_threshold -> eventflow
A visual representation of how the event separation works, can be seen in Figure 2.2-1.

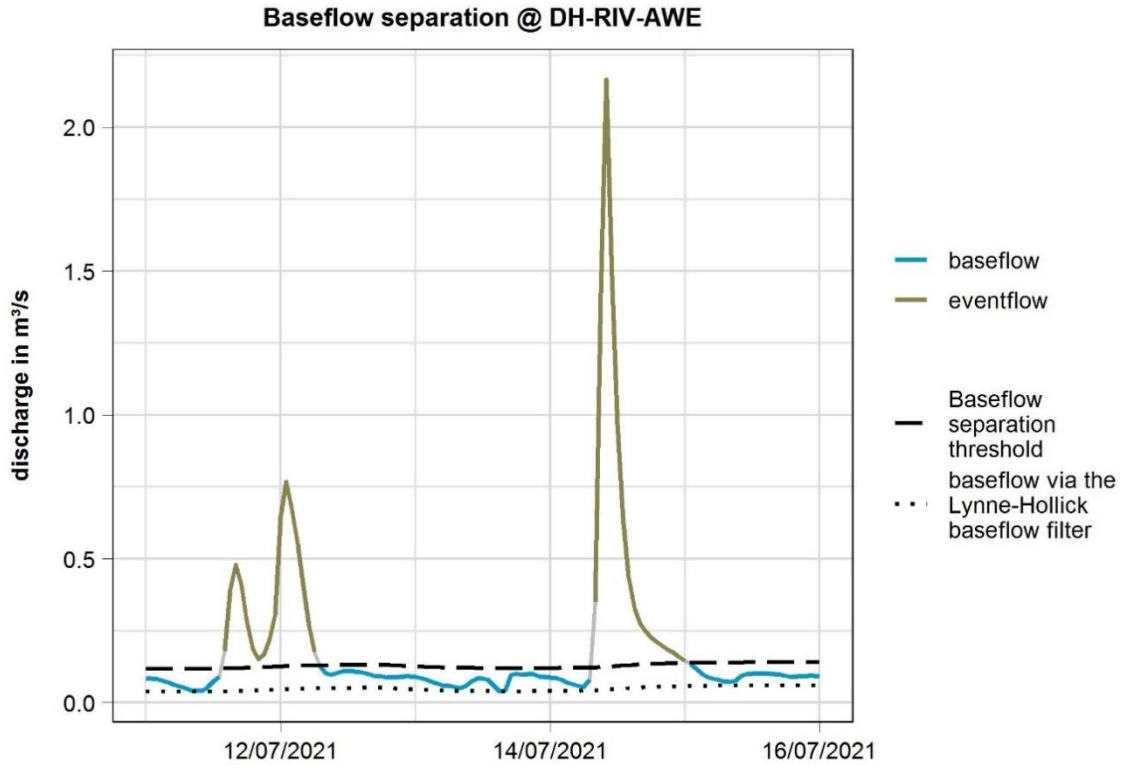

Figure 2.2-1 - River flow of Eisbach station (AT) with the final separation of flow condition (khaki = eventflow, blue = baseflow). With the baseflow river flow by Lynne-Hollick baseflow filter (dotted line) and the baseflow separation threshold (dashed line) timeline.

Baseflow separation results

River flow conditions have very strong consequences on both the measured concentrations and the loads calculated from it. It is important therefore to see, whether the sampled period represents average conditions or a dryer or wetter year. On Figure 2.2-2, a comparison of actual measured versus calculated long term average river loads for all stations included in our monitoring campaign. For most stations (16 out of 20) the actual year produced a slightly dryer than average condition, while at 2 stations (two stations at Vit catchment) somewhat wetter condition was sampled. The more significant deviation was experienced at Nodbach (Wulka), Upper Koppány, Upper Zagyva and also Zagyva outlet and at the middle station of River Somes (Figure 2.2-3). In terms of the share base flow index (BFI = ratio of annual average baseflow to annual average river flow), the distribution among the catchments is inhomogeneous (Figure 2.2-4). The highest BFI was experienced at stations with the highest share of waste water discharge (Upper Koppány, two stations at Wulka and the Tarján creek at Zagyva). At sites with larger upland catchments and more natural conditions (Somes, Vit and Ybbs) the share of eventflows are much higher, resulting a lower BFI (0.2-0.5). This fact

puts emphasis on the pathways that are related to rainfall-runoff processes. These are the runoff driven erosion, combined sewer and storm water system overflows. One smaller sidestream of the Zagyva (HZH) shows extremely high BFI, due to very small dry weather flows and relatively large runoff volumes.

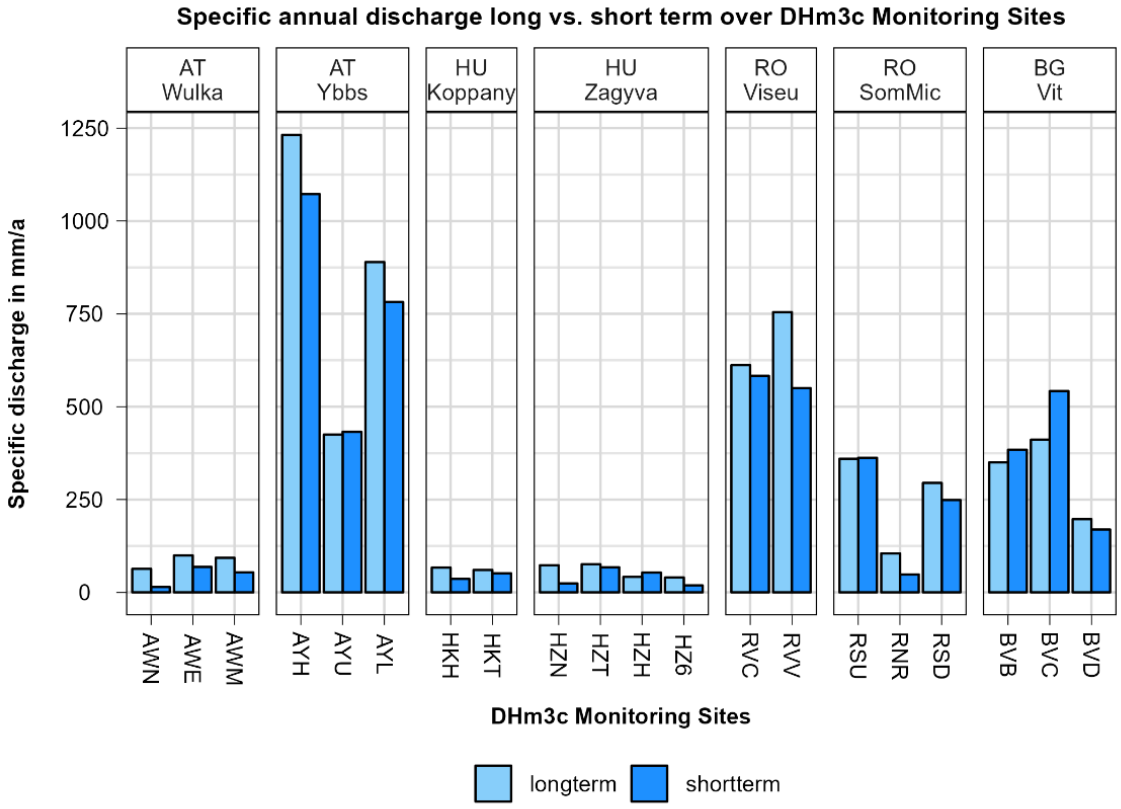

Figure 2.2-2 - Specific annual river flow long vs short term over the 20 DHm3c river monitoring stations.

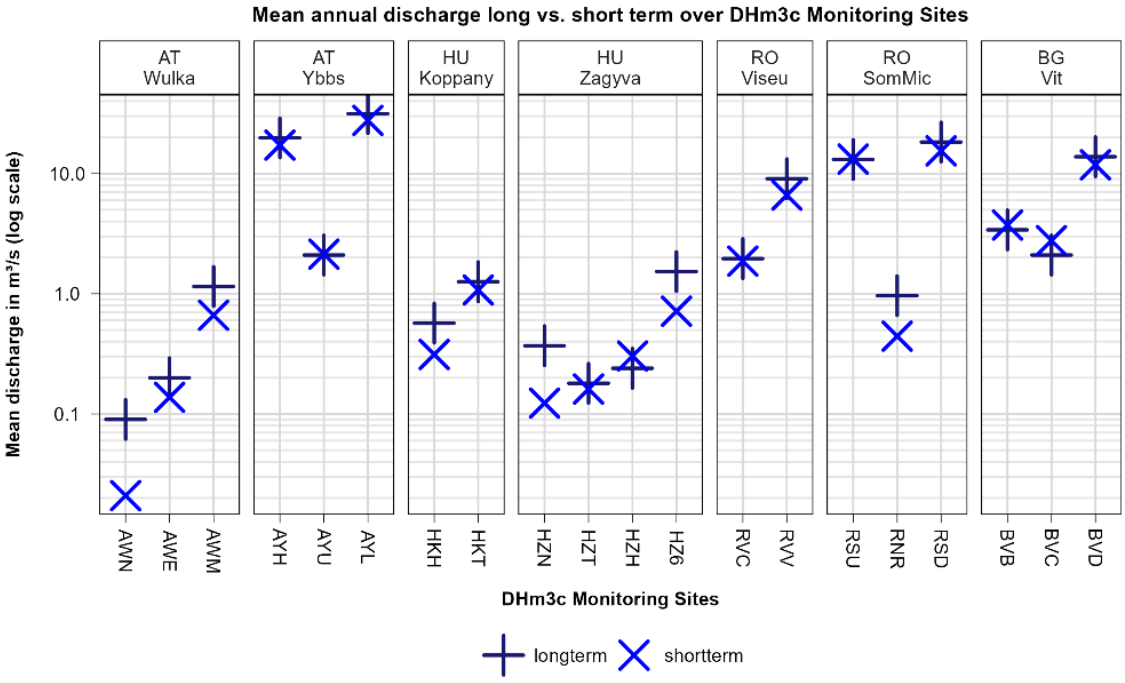

Figure 2.2-3 - Mean annual river flow (long vs. short term) over the 20 DHm3c river monitoring stations.

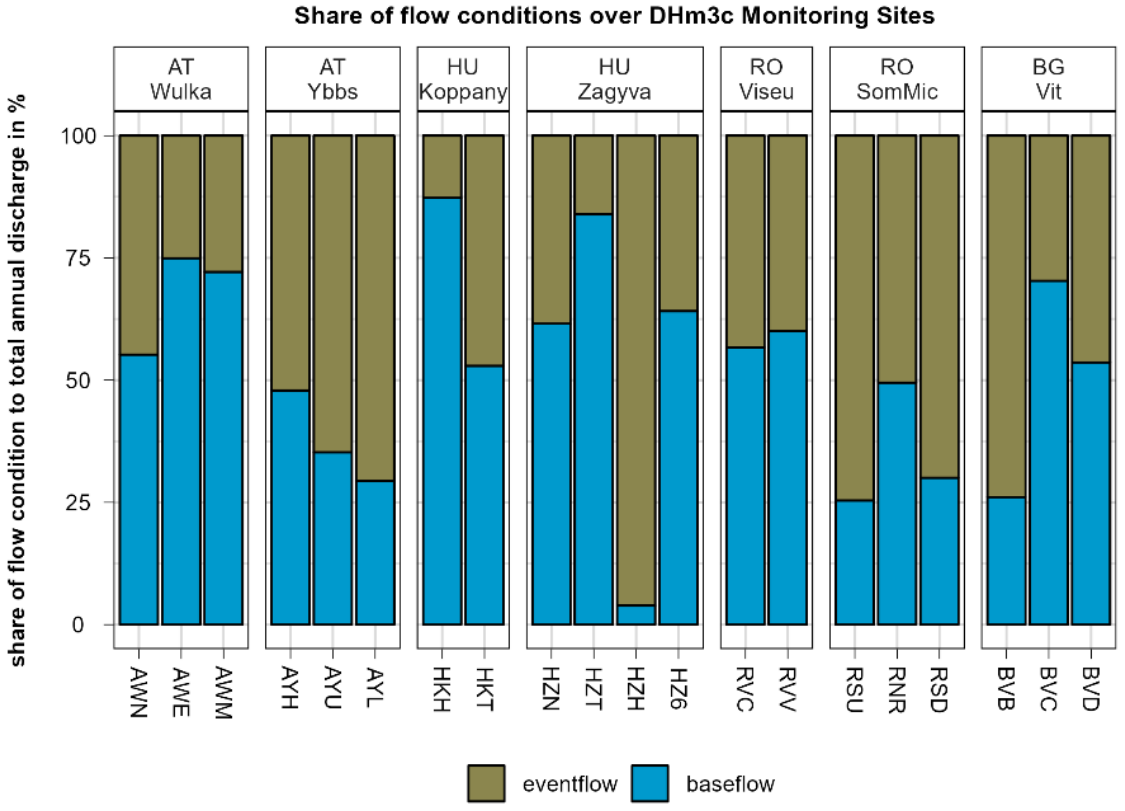

Figure 2.2-4 - Role (share) of the two flow conditions in yearly delivered water amount over the 20 DHm3c river monitoring stations.

Processing of concentration measurement data

The concentration data collected during the DH m³c monitoring campaign have been analysed. The composite samples have been taken under various flow condition which can be classified into two flow conditions: baseflow (low-flow to mid-flow(MQ)) and eventflow (high-flow). The eventflow is characterized by increased transport of suspended particulate matter. For detailed information about how the flow conditions during sampling were defined, see the DHm³c Output O.T1.2.

All samples were analyzed for total substance concentration of 47 micropollutants. Additionally, for heavy metals, dissolved concentration was analyzed by filtering the samples with 0.45 µm filters.

To avoid a bias in the calculated loads caused by outliers, average concentrations per substance, station, and matrix type (total or filtered) and flow condition was calculated. To be robust against single outliers with the rather small sample numbers, the median was chosen to calculate the average concentrations. As we are dealing with micropollutants, where environmental concentrations often occur around the lower limit of the analytical range of the available lab methods, for many substances a significant share of measurements are below the analytical LOQ (limit of quantification/quantitation), hence the data is partly censored.

To calculate statistical descriptor from censored data, we used the “ros” function from the R package “NADA” (Version 1.6-1.1). “ROS” stands for “Regression on Order Statistics” and is the “state-of-the-art”-method to deal with censored data (Helsel, 2012). The limiting factor is that the method only performs a reasonable calculation under these two conditions:

- There are at least 3 uncensored values (above LOQ)
- At least 20% of data is above LOQ.

The median concentration was based on one of the below methods, depending on the available data (first to last):

1) Value per flow condition (ROS)
2) Value for all samples (ROS)
3) Highest LOQ (equal to maximum evaluation)

Wherever possible, the median was calculated using ROS, but for those cases where this was not possible, a worst-case evaluation was chosen. To be consistent, the method is the same within each combination of substance, station, and matrix type (total or filtered).

In the case where there are, for each flow condition, enough measurements above the LOQ, the average concentration is calculated with ROS based on the flow condition, this reflects case 1 and is shown in Figure 2.2-5. Figure 2.2-5 shows the other two cases. For total matrix baseflow, only 1 value is above LOQ, so ROS can’t calculate a median value by the flow condition. Therefore, all samples are used, and because there are now 4 values above LOQ, ROS can calculate the median.

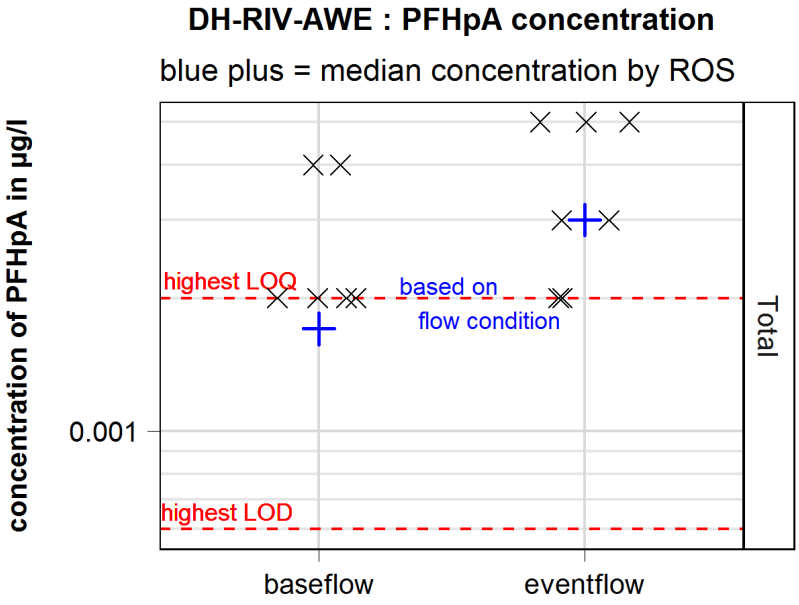

Figure 2.2-5 – Example 1: Concentration of PFHpA per flow condition for sample matrix total. All measurements are plotted as X-points. Plus-points show the median concentration and the text shows the source, which indicates that the median concentration is calculated by ROS for each flow condition.

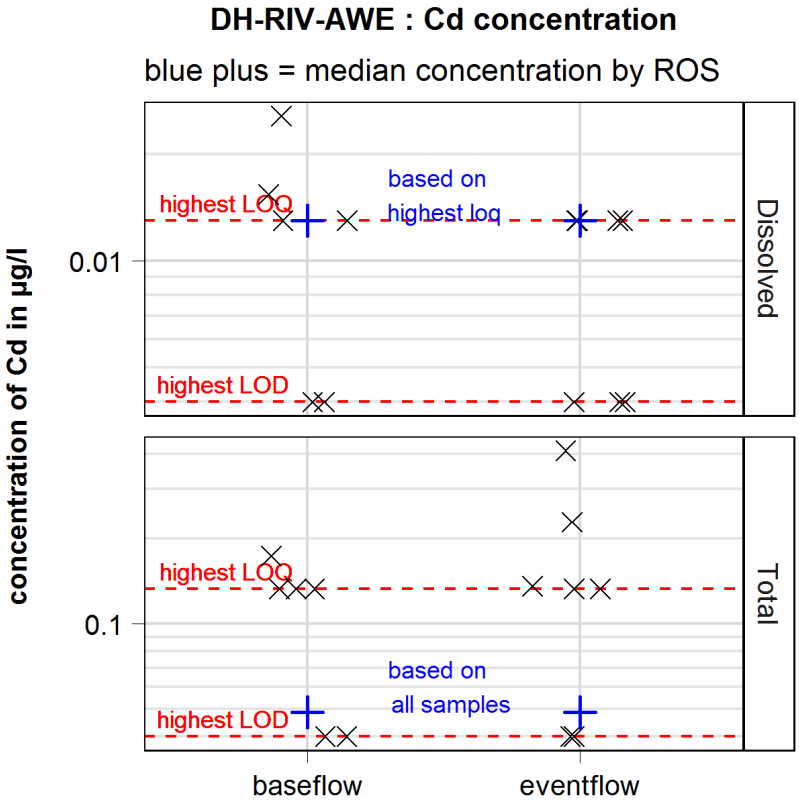

Figure 2.2-6 – Example 2: concentration of Cadmium (Cd) per flow condition and sample matrix. All measurements are plotted as X-points. Plus-points show the median concentration and the text shows the source.

The annual loads were also used to validate the results of the MoRE model. As the results come with an uncertainty, a different approach is used. The conditions on how to calculate the concentration is shown in Table 1.

Table 1 - Different conditions on how to calculate the concentration for MoRE Model Validation

Source	**Concentration by ROS**	**Concentration from LOQ**
Lower threshold	25th percentile	0
Median threshold	50th percentile	Highest LOQ/2
Upper threshold	75th percentile	Highest LOQ

Load calculation methodology

Method 1: "simulated grab sampling"

National hazardous substances monitoring is often done by taking 6-12 grab samples per year in equidistant time steps without consideration of the flow situation. Due to the more frequent occurrence of low- to mid-flow conditions, the chance that the low frequency grab samples are received during such situations is very high. To compare the resulting loads from the flow stratified sampling to loads from traditional sampling a second approach was applied. To calculate the loads, only the median concentration of the baseflow samples is used. The load per timestep is converted into load per year and then averaged. With this method we avoid dealing with data gaps in the river flow dataset (gaps can be up to a few weeks).

$$L_{BFonly} = \frac{1}{n} * \sum_{i=1}^{n} \left(\hat{c}_{BF} \times Q_{i,timestep} \times CU \right)$$

Form. 3.2-1.

CU conversion factor to convert the calculated values into a specific unit (annual loads)
L annual river load
n number of all timesteps
$\hat{C}$ contaminant concentration (M/L³)
Q_j mean hourly river river flow (L³/T) at the *i*th timestep
L length
M mass
T time

Method 2: using the advantage of stratified sampling

The load calculation method was developed to fit to the flow-stratified DHm³c monitoring campaign strategy (Output O.T1.2).

The pre-processed concentration data was merged into the pre-processed flow data according to the flow condition, matrix type, substance and station name. Then a load per timestep is

calculated by multiplying the river flow with concentration and a conversion factor, as shown in Form. 3.2-2.

The load per timestep was converted into load per year and then averaged. With this method, we can overcome the problem of data gaps in the flow dataset (gaps can be up to a few weeks). The annual load for each flow condition was then reduced to the actual share of the flow condition to reflect the actual distribution throughout the year. Both loads were then summed up to get the annual load. This can be written in a mathematical formula:

$$L_{BF+EF} = \frac{s}{n} * \sum_{i=1}^{n} \left(\hat{C}_{BF} \times Q_{i,\mathrm{BF}} \times CU\right) + \frac{(1-s)}{m} * \sum_{j=1}^{m} \left(\hat{C}_{EF} \times Q_{j,EF} \times CU\right)$$

Form. 3.2-2.

where

CU	conversion factor to convert the calculated values into a specific unit (M/T)
s	share of baseflow river flow to total river flow [0,1]
n	number of baseflow timesteps
m	number of eventflow timesteps
L	annual river load
$\hat{C}$	median contaminant concentration (M/L³) (subscript indicates flow condition)
Q_i	mean hourly river river flow (L³/T) at the i^{th} timestep
BF	baseflow
EF	event flow
L	length
M	mass
T	time

Method 3: Involving online turbidity measurements and TSS concentrations

The most developed method makes use of the TSS measurements the partners conducted on their premises as well as of the online (inline) turbidity measurements. In addition to the online tubidity measurements (results delivered by the online probes are usually in FNU), some partners also did turbidity measurements of the grab samples in their labs (results delivered in NTU). The third quantity used to describe the turbidity / suspended solids content of a sample is it's TSS concentration (Figure 2.2-8**).**

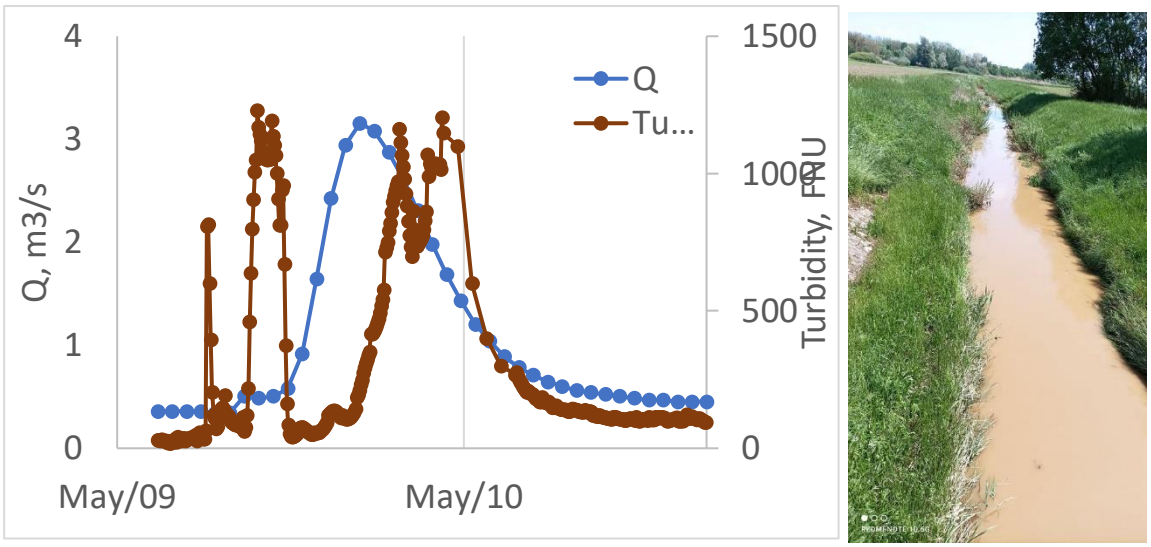

Figure 2.2-7 – Graph and photo of an example runoff event at Törökkoppány Koppány-creek, Koppány pilot region in May 2022. Qmax = 3.15 m3/s ≈ Q 1% = 3.35 m3/s . TSS = 16 160 mg/l

The steps of the data evaluation were as follows:

1. Establish the correlation between total suspended solids (TSS) concentration and turbidity;
2. Evaluate the relationships between TSS concentration and the concentrations of potentially sediment-bound contaminants (nutrients, PTEs);
3. Development of SS loading generator based on continuous (online) turbidity data;
4. With the application of flow separation, estimating the contribution of the high-flow events to river loads.

This method was applied on the 6 Hungarian river monitoring stations.

Results of load calculation

The correlation between TSS and turbidity is enough strong for the development of a rating curve, and there are no significant differences in the sampling sites (*Figure 2.2-8*).

Outliers were supported by lab analysis of the suspended matter. When the sample has very high colloid content, the turbidity measurment overestimates the TSS concentration. These conditions occur when rain falls on soils after long dry periods or less freshly washed-off material is resuspended from the riverbed. Freshly eroded soil causes high sand content, which is poorly approximated by turbidity due to rapid sedimentation.

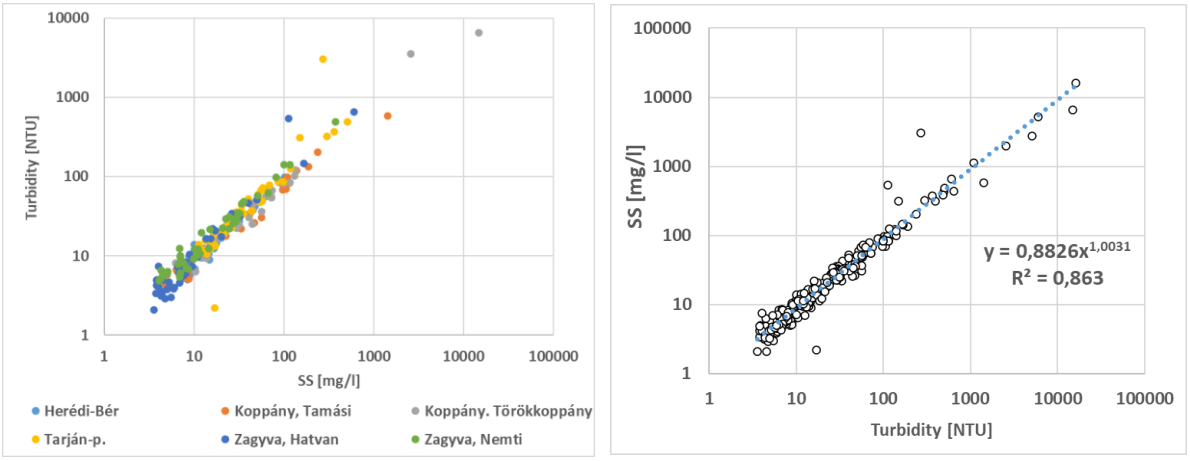

Figure 2.2-8 – Relationship between SS concentration and Turbidity by sampling sites and rating curve fitted to all points

Sediment load was derived directly from high frequency online turbidity data, by using the TSS = f(turbidity) function. After flow separation (e.g. with the application of Q_{10}% threshold) the contribution of the high-flow events to total SS river load can be estimated.

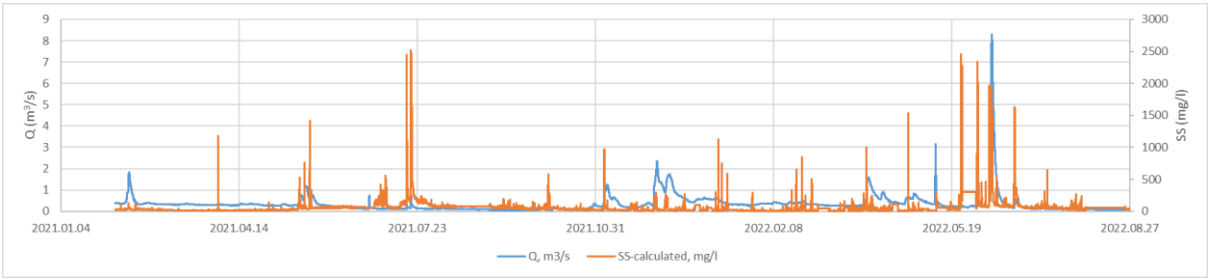

Figure 2.2-9 – Time series of SS generated from high frequency turbidity measurements (Station Törökkoppány)

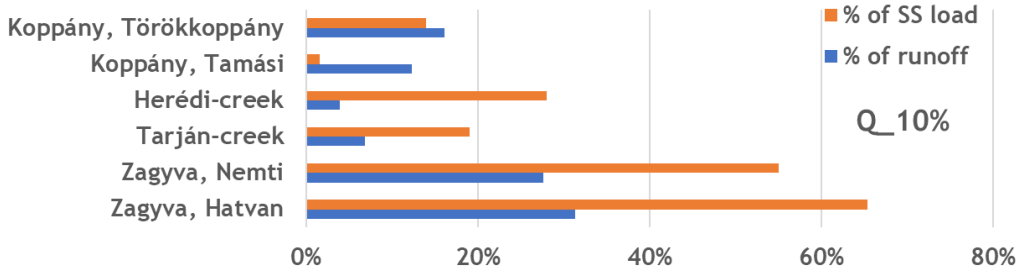

Figure 2.2-10 – Contribution of high flow events to the total runoff and SS load

Linearly correlated relationship between SS concentration and some of the potentially sediment-bond contaminants (As, Cu, Pb, Zn) can be observed (*Table 3*), and according to the expectations there is no correlation with dissolved concentrations.

Table 3 - Pearson correlation between concentrations of contaminants and SS concentration.

Substance	r^2	Pearson correlation
Turbidity	0,855	0,925
As_total	**0,823**	**0,907**
Cd_total	0,391	0,625
Cr_total	0,019	0,138
Cu_total	**0,705**	**0,840**
Hg_total	0,104	0,322
Ni_total	0,008	0,092
Pb _total	**0,517**	**0,719**
Zn_total	**0,651**	**0,807**
As_dissolved	0,020	-0,141
Cd_dissolved	0,000	0,016
Cr_dissolved	0,002	-0,041
Cu_dissolved	0,033	0,182
Hg_dissolved	0,058	0,242
Ni_dissolved	0,000	-0,001
Pb _dissolved	0,005	0,070
Zn_dissolved	0,036	-0,190

Results highlighted that in case of the majority of substances (except some metals), the correlations are not strong enough to estimate the substance load from the suspended solids content. Therefore, calculation of river load happened with following formula (in accordance with the stratified river sampling method).

If $Q < Q_{10\%}$ $L_{lowflow} = \Sigma (Q_i * C_{composite})$

If $Q > Q_{10\%}$ $L_{highflow} = \Sigma (Q_i * C_{flow\ event's\ average})$

Where Q stands for river dischargem $Q_{10\%}$ refers to 10 % exceedance probability discharge, C refers to concentration of the contaminant.

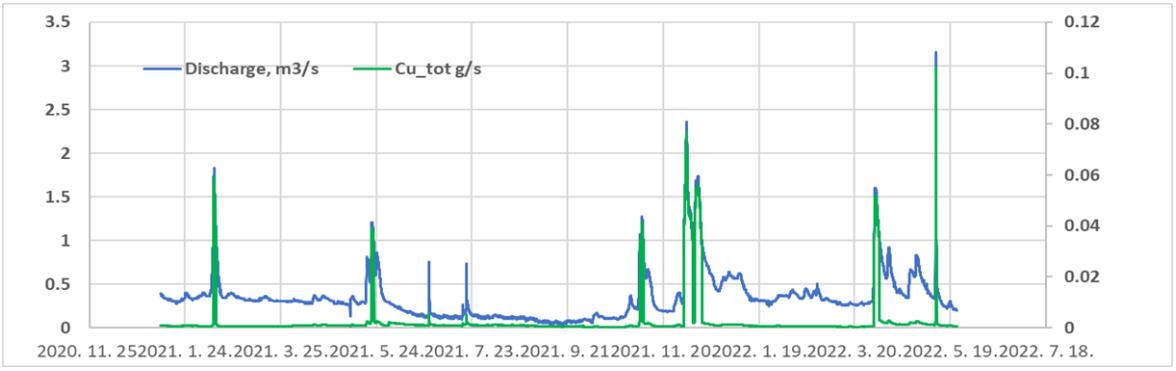

Figure 2.2-11 – Time series of water flow (left vertical axis) and assessed total Cu loads (right vertical axis) at Törökkoppány, Koppány pilot region.

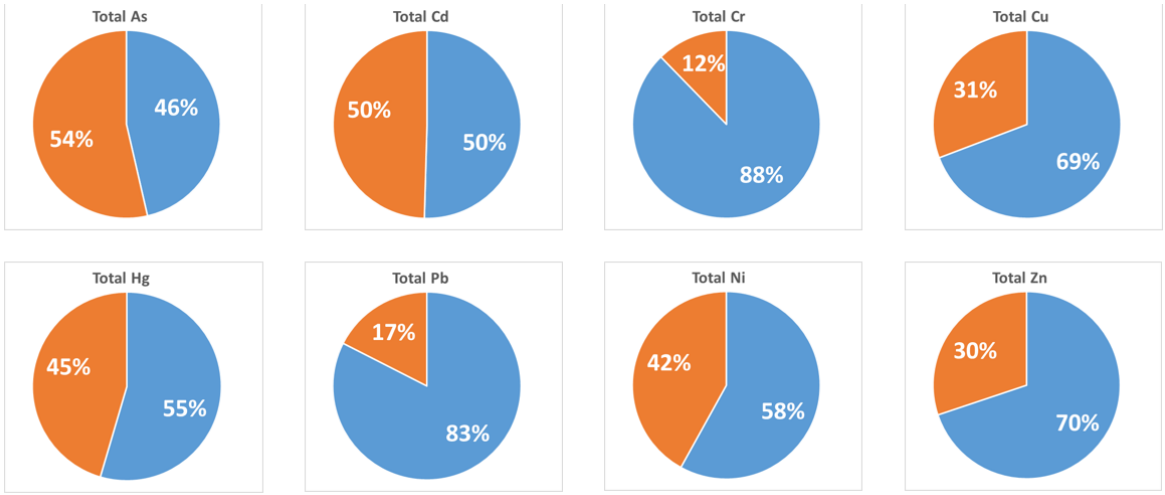

Figure 2.2-12 – Assessed low- and high flow HM loads at Törökkoppány

The results of this method can be concluded as follows. High-flow events might deliver up to 70% of the annual SPM load while delivering only 15-35% of the total yearly runoff. Concentrations of potentially toxic metals and particulate P significantly elevated in high flow events. Flood events have a significant role in all sediment-bound contamination transport in river systems, therefore skipping high flow events from regular monitoring can result in significant underestimation of river loads. Stratified sampling (separation of different hydrological situations) could be a cost-effective approach for river monitoring. Online measurement of turbidity can be used to refine sediment load estimation. Further efforts are needed to identify the sources of contaminants (soil, wastewater, sediment release, etc).

Industrial chemicals

PFOS is shown here as example for industrial chemicals, , as it was detected in most of the pilot regions (Figure 2.2-13). Especially the areas with high population densities (Wulka in Austria, Upper Zagyva below Salgótarján WWTP effluent and Somes below the effluents of Cluj Napoca WWTP) and low dilution factors show elevated values above the EQS (Environmental quality standard).

The Austrian catchments and one Romanian station have the highest specific loads (Figure 2.2-14). Catchments with very low population densities (Viseu: RVV, RVC, Vit: BVB, BVC, Ybbs: AYH) show very high uncertainties because those loads could only be calculated using LOQ-concentration, hence it can be considered as worst-case scenario.

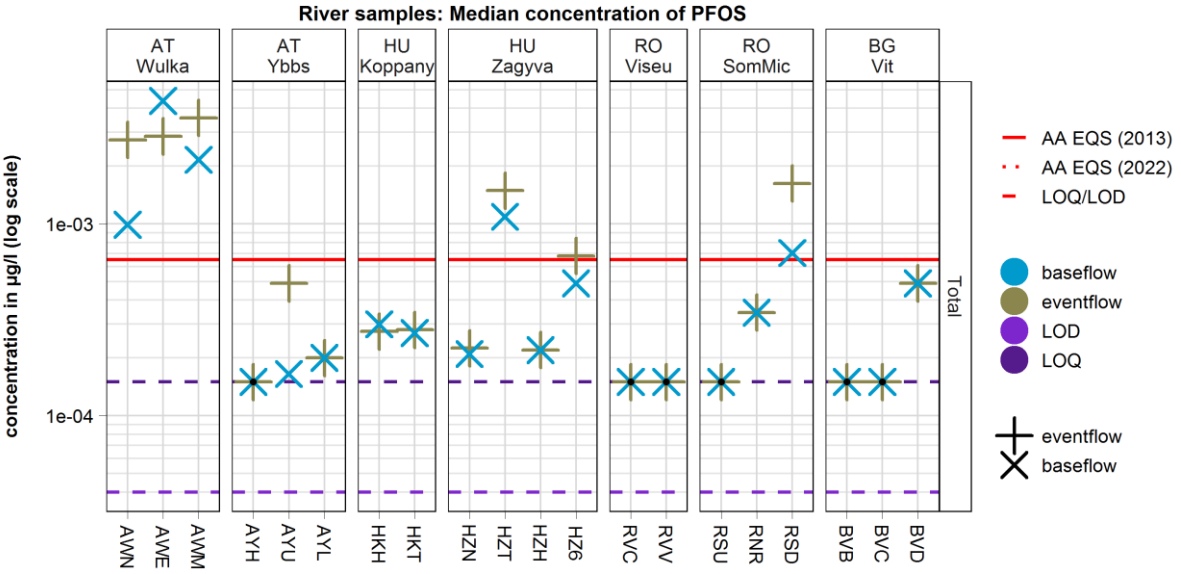

Figure 2.2-13 - Median concentration of PFOS used for the load calculation. Concentrations for both flow conditions with LOQ/LOD and the AA EQS

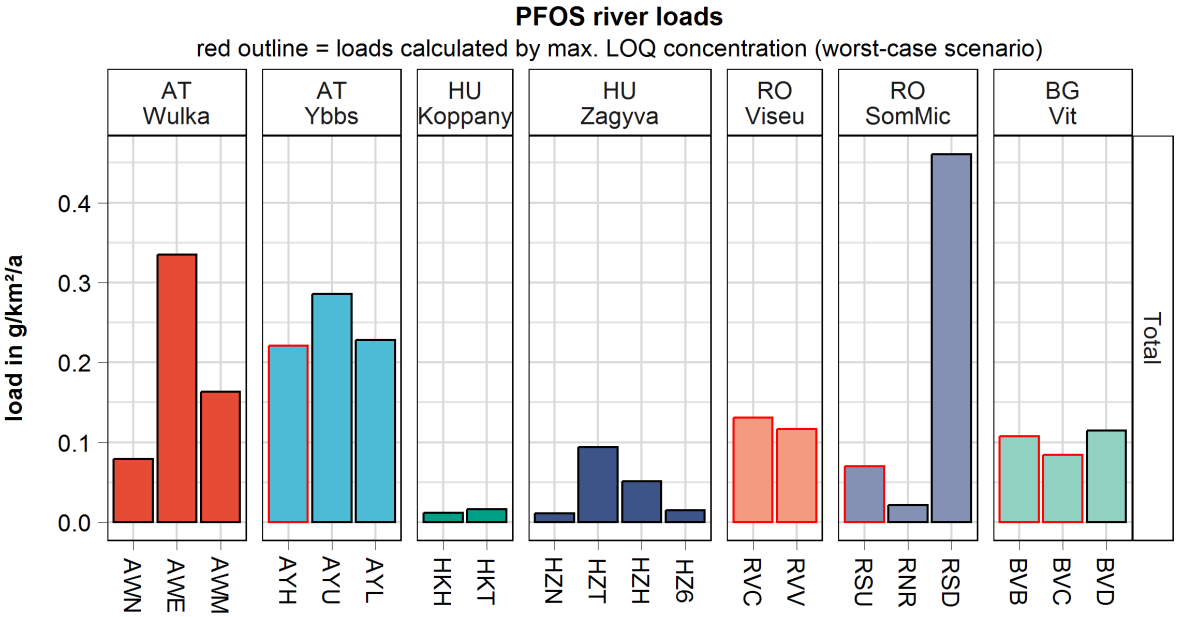

Figure 2.2-14 - Specific annual river loads of PFOS. Columns with red outline are loads calculated by max. LOQ (worst-case scenario).

Pharmaceuticals

Diclofenac, as an example for pharmaceuticals, is an indicator for anthropogenic pollution, related mostly to WWTP effluents and combined sewer overflows. The measured concentrations of Diclofenac (Figure 2.2-15) are up to 2 order of magnitudes above the newly proposed EQS threshold in the higher populated pilot regions.

The influence of WWTP effluent for diclofenac is, as expected, clearly visible in Figure 2.2-16. For example the Stations “AWE” and “AWN” have approx. the same size upstream catchment but “AWE” is downstream of a big town with WWTP, and “AWN” has no WWTP inflow. The loads are by an order of magnitude higher for the WWTP influenced station “AWE”. This confirms that sewage treatment plants are a major source of this pharmaceutical. However, diclophenac was also detected at “AWN”, albeit in low concentrations. This means that there are also other diffuse sources of diclofenac. By comparing the specific loads over the disposing inhabitants, increasing loads with increasing disposing inhabitants’ density can be observed, as shown in Figure 2.2-17.

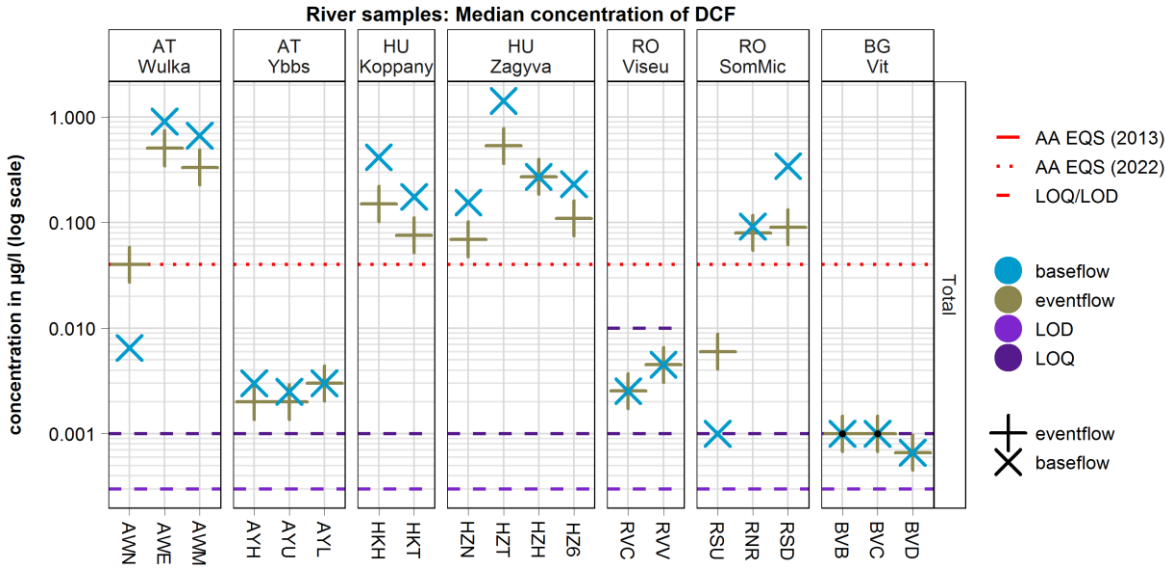

Figure 2.2-15- Median concentration of Diclofenac used for the load calculation. Concentrations for both flow conditions with LOQ/LOD and the AA EQS

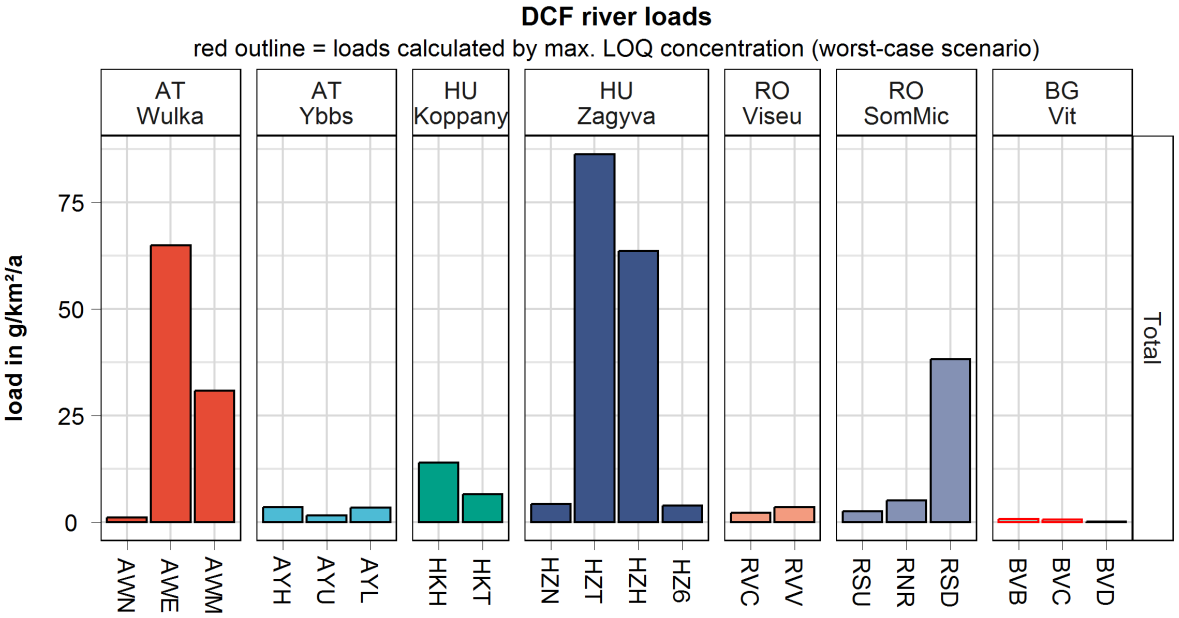

Figure 2.2-16 - Specific annual river loads of Diclofenac. Columns with red outline are loads calculated by max. LOQ (worst-case scenario).

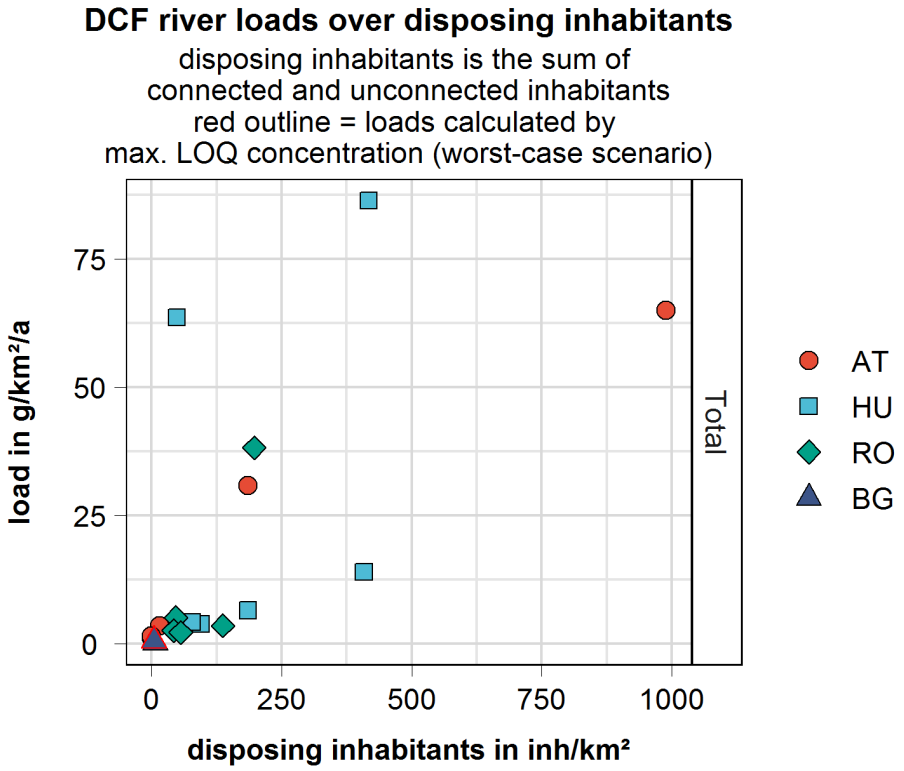

Figure 2.2-17 - Specific load over disposing inhabitants density for the substance diclofenac. Colour indicate the country of the station.

Heavy metals

Nickel and Zinc are shown here as examples for the behaviour of heavy metals.

The observed nickel median concentrations for the dissolved fraction are below the current EQS, but with the new proposed EQS some rivers would exceed this threshold as seen in Figure 2.2-18. For the total fraction, the eventflow concentrations are about 0.5 to 1 order of magnitude higher than for baseflow throughout the pilot regions. This is supported by the literature (See Metals part in Chapter 1.1).

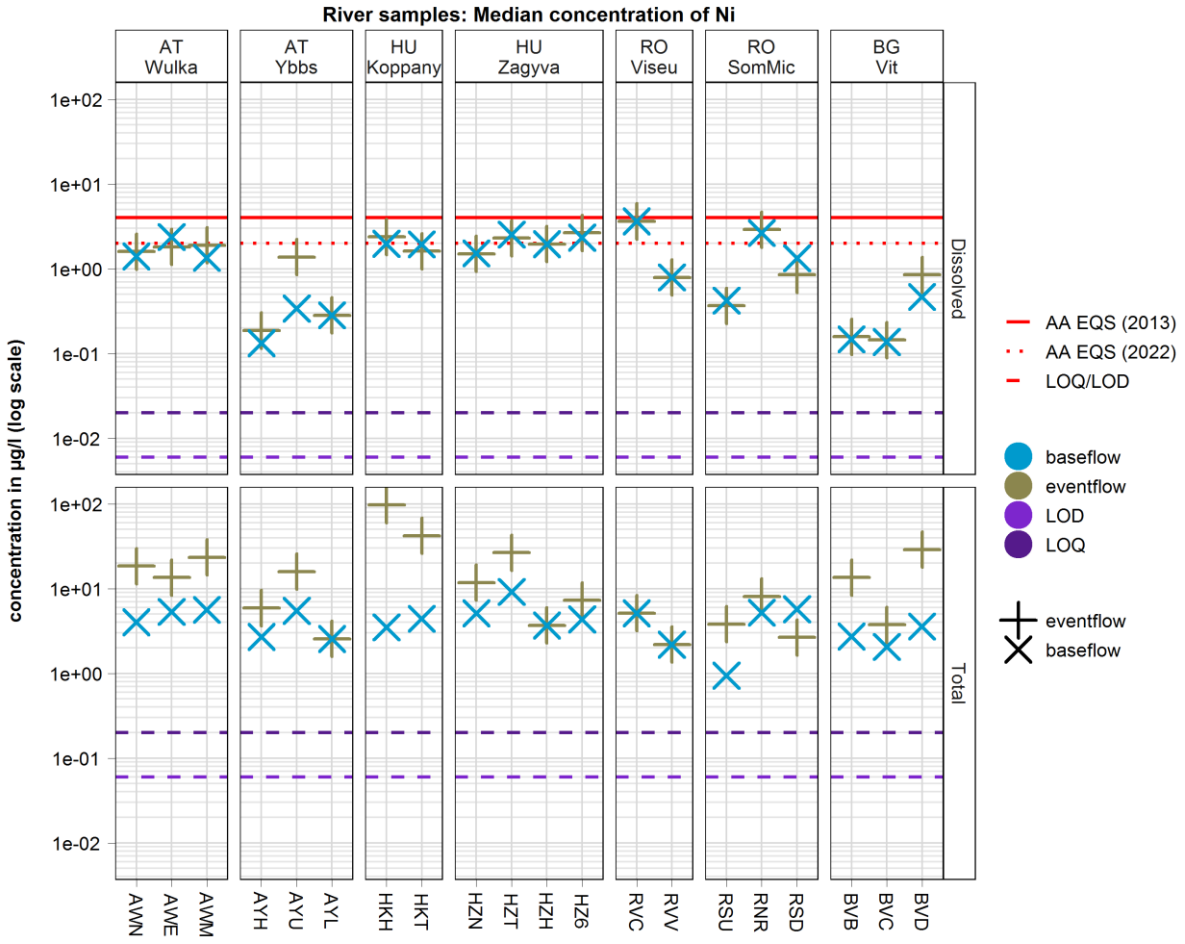

Figure 2.2-18 - Median concentration of Nickel used for the load calculation. Concentrations for both flow conditions and sample matrixes with LOQ/LOD and the AA EQS

The specific loads in **Hiba! A hivatkozási forrás nem található.** Figure 2.2-19 reveal a heterogeneous distribution of loads throughout the pilot regions. For the dissolved fraction, the Romanian mining catchment stands out, clearly indicating the elevated background concentrations from the mining sites. In case of total fraction the Austrian Ybbs and Bulgarian Vit catchments show the highest specific loads. This is due to geogenic sources and high specific river flows. The specific loads of zinc are extremely high for the mining areas in Romania, see Figure 2.2-20. This is the same case for As, Cd, Cu, Pb.

Conventional monitoring approaches for an EQS-based assessment with e.g. monthly grab samples miss situations with high concentrations of total suspended solids (TSS) and

associated chemicals. This is a clear shortcoming, especially in the context of load observations. **Hiba! A hivatkozási forrás nem található.**

Figure 2.2-21 emphasises this by showing the importance of eventflow sampling for the heavy metal nickel. Loads are underestimated by half when eventflow is not taken into account.

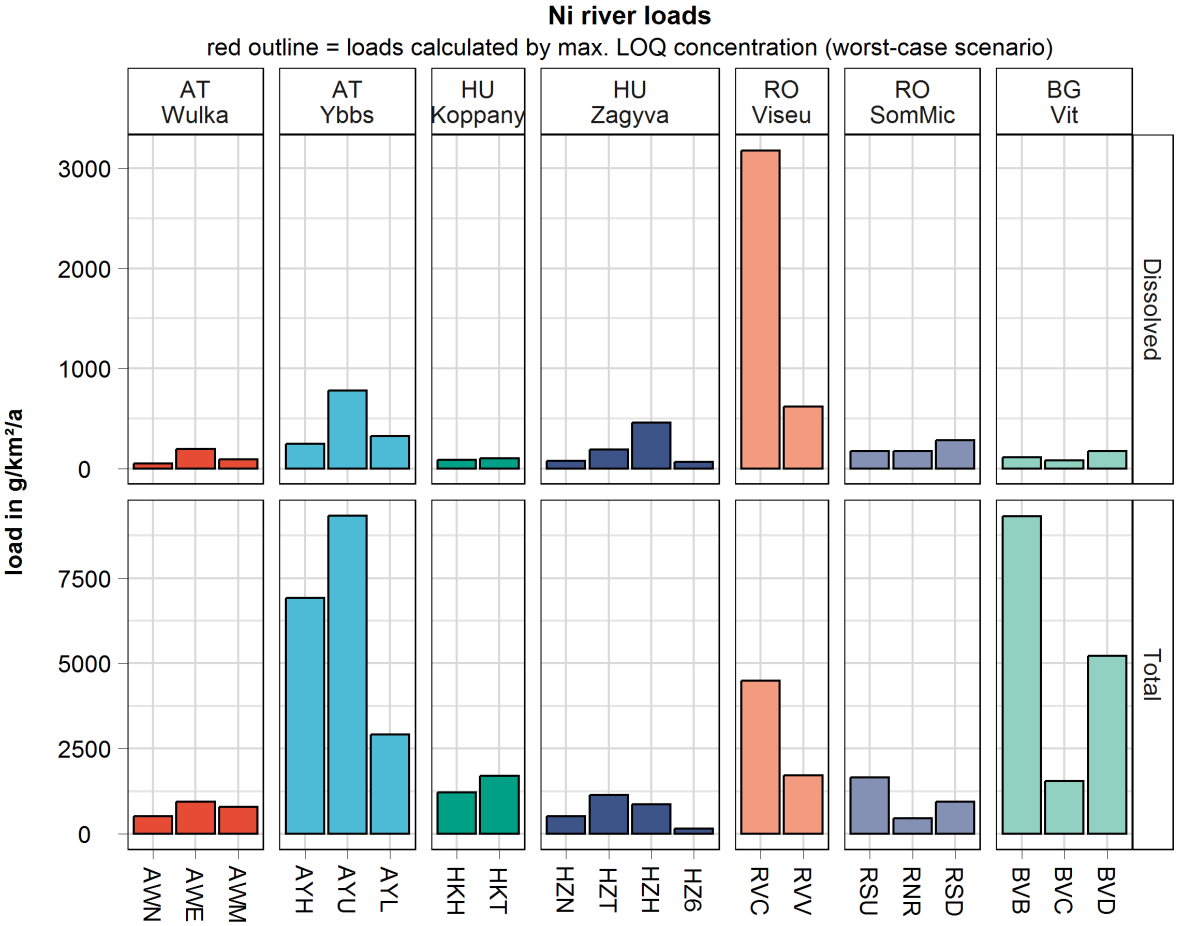

Figure 2.2-19 - Specific annual river loads of nickel for both sample matrixes. Columns with red outline are loads calculated by max. LOQ (worst-case scenario).

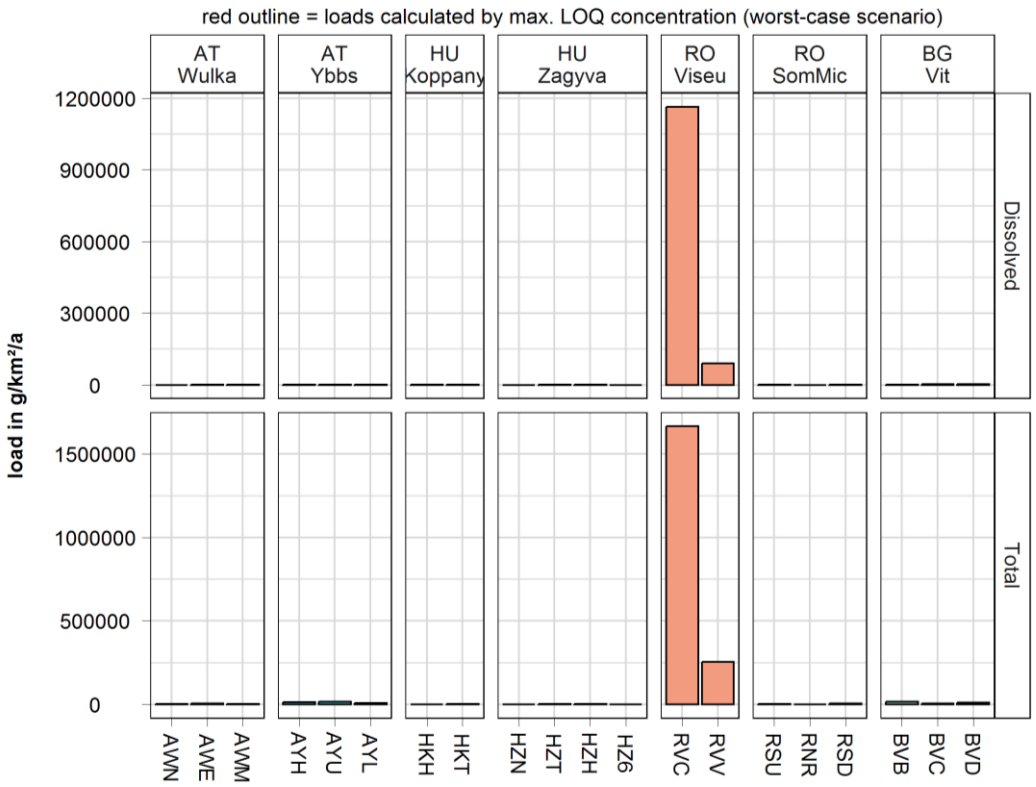

Figure 2.2-20 - Specific annual river loads of zinc for both sample matrixes. Columns with red outline are loads calculated by max. LOQ (worst-case scenario).

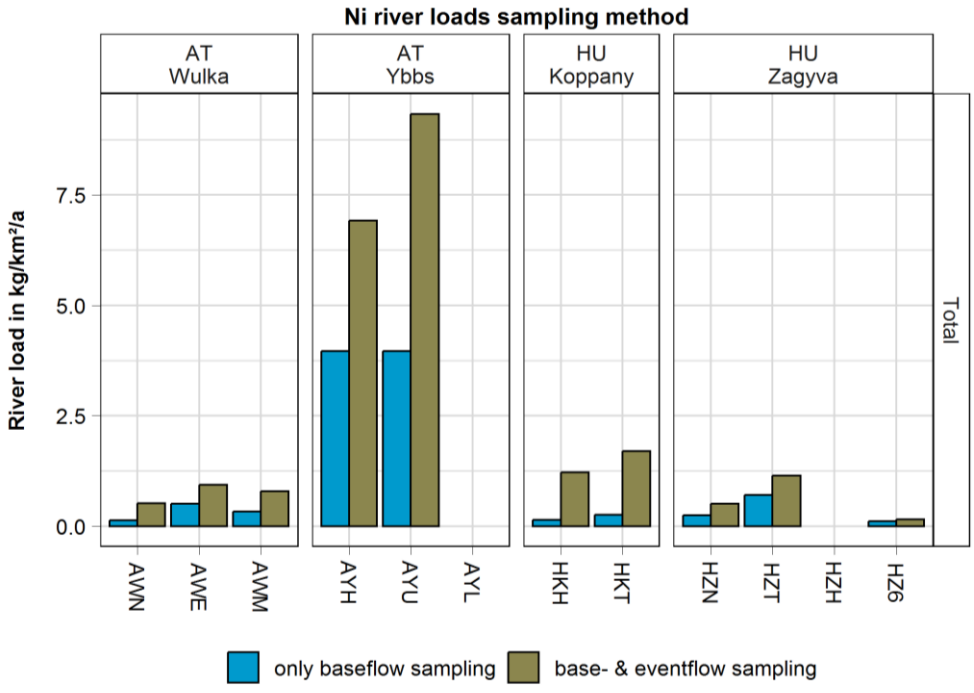

Figure 2.2-21 - Comparison of load calculation methods. Blue bars show specific loads calculated only with baseflow samples and brown bars the specific loads calculated with both baseflow and eventflow samples.

Pesticides

Metolachlor ethanesulfonic acid (Metolachlor ESA) is a metabolite of the herbicide Metolachlor. It is found in the river waters throughout the pilot regions in various concentrations, see Figure 2.2-22, which is likely due to the strongly varying application rates across the regions. With regard to specific loads (Figure 2.2-23), the catchment "AYU", which is dominated by agricultural land use, stand out due to relative high concentrations and specific river flows compared to the other regions. Load estimation comparison (Figure 2.2-24) show differences for the Ybbs and Koppány catchments, the two most polluted rivers at least based on concentrations. While for the Ybbs the differences in annual loads are marginal by the comparison, for Koppány catchment, the there is a twofold underestimation if highflow loads are neglected. This is coming from the fact that in the Ybbs the highflow and low flow concentrations are in the same range (quite unexpected result), while at the Koppány, there is a large difference in the concentrations when sampling the two strata (high-turbidity samples might explain this large deviation). This highlights the unique circumstances found in catchments.

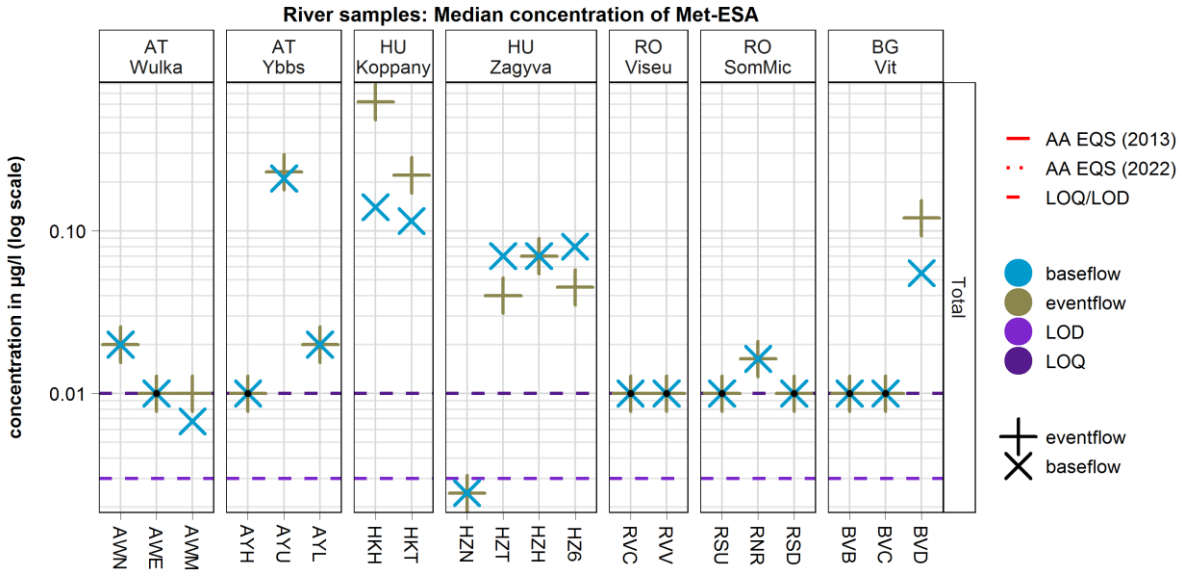

Figure 2.2-22 - Median concentration of Metolachlor ESA used for the load calculation. Concentrations for both flow conditions and sample matrixes with LOQ/LOD and the AA EQS

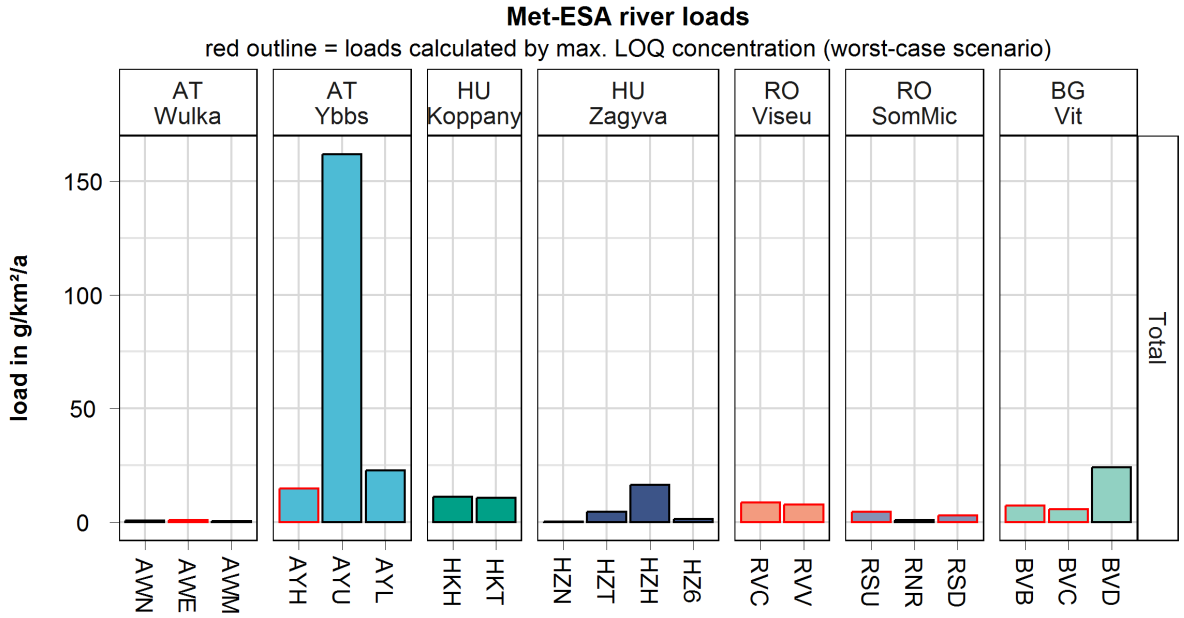

Figure 2.2-23 - Specific annual river loads of Metolachlor ESA. Columns with red outline are loads calculated by max. LOQ (worst-case scenario).

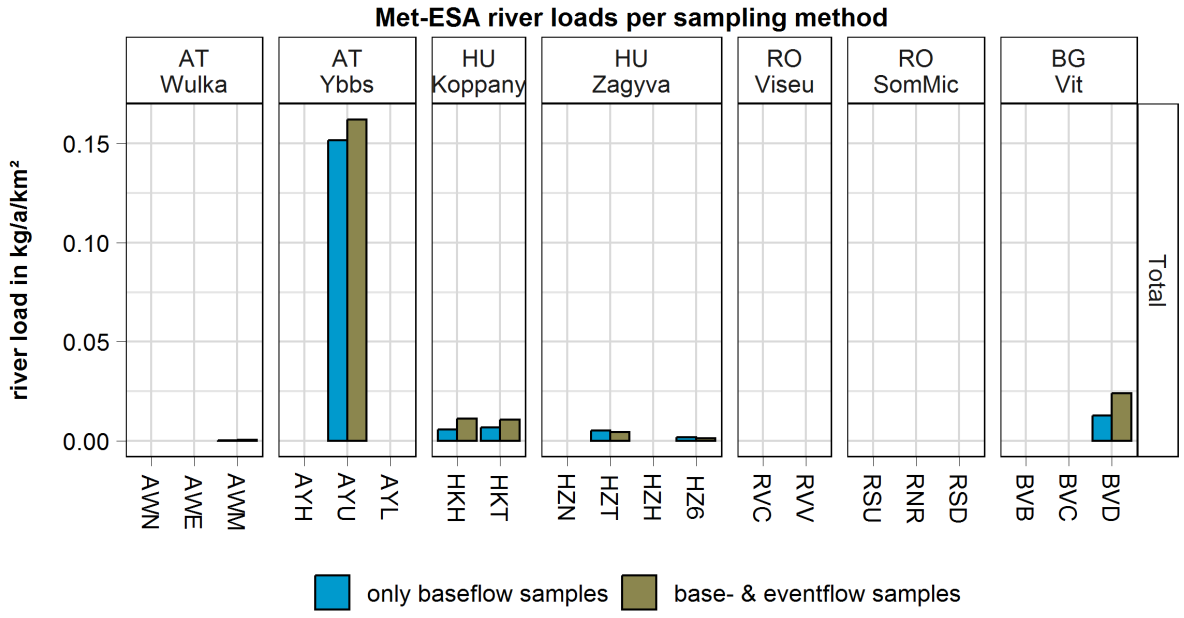

Figure 2.2-24 - Comparison of load calculation methods. Blue bars show specific loads calculated only with baseflow samples and brown bars the specific loads calculated with both baseflow and eventflow samples.

3 CONCLUSIONS

Heavy metals in rivers

Some extremely high HM values were detected in river high flows, even outreaching concentrations measured in wastewaters (in case of As, Cr, Cu, Ni, Pb, Zn), which clearly

indicates that these originate (at least partly) from diffuse sources and are washed off / resuspended during surface runoff/higher river flow conditions (high flow events).

PAH

One possible explanation for lower molecular weight PAH forms occurring more often in aqueous samples and less often in soil samples is that they show lower hydrophobicity, the threshold seems to be around log k_{OW} = 5.5.

Load calculation

Discharges during sampling were lower than average, except for the two headwaters in the Bulgarian basin, and the sidereach of the Ybbs River and the Somes above Cluj Napoca. A large variation of area-specific loads was observed for most substances across the catchments. This variability is likely to be related to the large differences in catchment characteristics and emissions. The large influence of waste water discharges and the high share of high-flow loads should be emphasized in this respect. Pharmaceuticals are good indicators of anthropogenic point sources in the catchment but it was found that they may also enter the waterways by diffuse pathways, which is a new finding of this project. The inclusion of high-flow events in the monitoring has a significant effect on annual load estimates in case of certain substances and catchments and should therefore play an important part of any sampling program. Mining sites effluents showed extremely high specific load values with respect to heavy metals (Cd, Cu, Pb and Zn) and arsenic. The varying occurrence of pesticides in the rivers indicate that their application rate varies strongly across the regions.

Data evaluation was completed by regression analysis and loading functions were developed. Results show significant differences in the event patterns among the sampling sites, however, the overall conclusions were as follows: heavy metals indicate high variability during high-flow events, and seem capable of differentiating between different hydrological circumstances.

The relationships between SS and the concentrations of sediment-bound substances (i.e. heavy metals and part of PAHs) was established. Based on the strong correlation between SS and on-line turbidity, the continuous time series of the sediment-bound contaminants were generated, and with the application of flow separation the contribution of the high-flow events to river load was estimated. Results induced that high-flow events might deliver up to 70% of the annual SS and contaminant load while delivering only 15-35% of the total yearly runoff. The results highlighted that flood events have a significant role in the case of all sediment-bound contamination transport in river systems.

4 ANNEXES

All measured concentrations and calculated loads can be found in Annex I (D.T1.2.3 - concentrations and loads.zip, containing several data sheets in excel format)

5 REFERENCES

Bond, N. (2022). *hydrostats: Hydrologic Indices for Daily Time Series Data. R package version 0.2.9* (0.2.9).

EC. (2022). *Proposal for a Directive of the European Parliament and of the Council amending Directive 2000/60/EC establishing a framework for Community action in the field of water policy, Directive 2006/118/EC on the protection of groundwater against pollution and d* (pp. 1–28).

Everitt, B. S., & Hothorn, T. (2003). A Handbook of Statistical Analyses using R. In *American Statistician* (Issue 1). https://doi.org/10.1198/tas.2003.s221

Gao, Y., Liang, Y., Gao, K., Wang, Y., Wang, C., Fu, J., Wang, Y., Jiang, G., & Jiang, Y. (2019). Levels, spatial distribution and isomer profiles of perfluoroalkyl acids in soil, groundwater and tap water around a manufactory in China. *Chemosphere*, *227*, 305–314. https://doi.org/10.1016/j.chemosphere.2019.04.027

Giménez-Forcada, E., Luque-Espinar, J. A., López-Bahut, M. T., Grima-Olmedo, J., Jiménez-Sánchez, J., Ontiveros-Beltranena, C., Díaz-Muñoz, J. Á., Elster, D., Skopljak, F., Voutchkova, D., Hansen, B., Hinsby, K., Schullehner, J., Malcuit, E., Gourcy, L., Szőcs, T., Gál, N., Þorbjörnsson, D., Tedd, K., … Rosenqvist, L. (2022). Analysis of the geological control on the spatial distribution of potentially toxic concentrations of As and F- in groundwater on a Pan-European scale. *Ecotoxicology and Environmental Safety*, *247*(April). https://doi.org/10.1016/j.ecoenv.2022.114161

Helsel, D. R. (2012). *Statistics for censored environmental data using Minitab and R* (2nd Ed.). Wiley.

Hepp, G. (2022). *DTSg: A class for workign with time series data based on "data.table" and "R6" with largely optional reference semantics. R package version 1.1.1* (1.1.1).

Ladson, A. R., Brown, R., Neal, B., & Nathan, R. (2013). A standard approach to baseflow separation using the Lyne and Hollick filter. *Australian Journal of Water Resources*, *17*(1), 25–34. https://doi.org/10.7158/13241583.2013.11465417

R Core Team. (2019). *R: a Language and Environment for Statistical Computing*. R Foundation for Statistical Computing.

Yang, Y., Ok, Y. S., Kim, K. H., Kwon, E. E., & Tsang, Y. F. (2017). Occurrences and removal of pharmaceuticals and personal care products (PPCPs) in drinking water and water/sewage treatment plants: A review. *Science of the Total Environment*, *596–597*, 303–320. https://doi.org/10.1016/j.scitotenv.2017.04.102